Final Progress Report

Innovative, Reliable Personal Monitors for Mine Worker Protection

CDC Grant # 1R01OH009548-01

SUBMITTED BY

2605 Trade Centre Ave, Suite C
Longmont, CO 80503

Tel: (720) 494-8401 •Fax: (720) 494-8402

October 29, 2010

Table of Contents

1. LIST OF TERMS AND ABBREVIATIONS

LEL - lower explosive limit
MOS sensor-metal oxide semiconductor sensor, synonymous with chemiresistor sensor
CGS - combustible gas sensor, synonymous with pellistor sensor
echem – electrochemical (amperometric) sensor
RS-MG detector – redundant sensor multi-gas detector
AAO – anodic aluminum oxide
ppm – concentration ratio by volume, expressed in units of part per million
MSHA – Mine Safety and Health Administration
ISA – Instrument Society of America

2. ABSTRACT

Coal mining is an extremely dangerous enterprise, with accidents over the past year in the U.S., Chile, China, and elsewhere making news headlines. Despite many recent technological enhancements, it remains one of the most hazardous occupations. One of the recurring challenges in mining is the potential of worker exposure to toxic gases (typically carbon monoxide), oxygen depletion, or the risk of explosions due to the build-up of combustible gases, such as methane. In this project, technology for monitoring of these gases with improved reliability has been developed with the ultimate goal of increasing the safety of mine workers. These improvements are enabled by an innovative approach involving the use of complementary sensors for measuring the same gas. These redundant sensors work in conjunction to overcome the inherent limitations of each sensor when operated alone, thereby ensuring higher reliability than is currently available from commercial multi-gas monitors. In this project, the redundant sensor approach was demonstrated by the construction and testing of a prototype *redundant sensor multi-gas (RS-MG) detector* for mine gases. A combination of microsensors developed at Synkera and commercially available electrochemical gas sensors were utilized. The microsensors developed and tested in this project take advantage of advances in nanomaterials and ceramic micromachining, which were used to create low-cost sensors that are miniaturized and operate at extremely low power. These features allow this redundant approach to be implemented in a manner that does not appreciably increase the size or cost of a multi-gas monitoring unit compared to currently available commercial units. With suitable low-profile packaging and further testing in the field, this technology should result in a next-generation personal gas monitor providing enhanced safety for mine workers.

3. SUMMARY OF FINDINGS AND IMPACT

Highlights

Although continuous improvements in methods, hazardous gas monitoring and ventilation have reduced many of the risks associated with the mining industry, mining remains the second most dangerous occupation in America according to the Bureau of Labor [1]. The mining industry routinely deals with adverse and hard to control natural and environmental conditions. The environmental conditions of greatest concern include the build-up of hazardous gases (such as combustible gases and carbon monoxide) and reduction of oxygen levels. Although fatalities related to gas explosions and/or fire would likely be prevented or reduced if *all* personnel were equipped with reliable personal gas detectors, the performance and cost of current portable instruments have been barriers to such deployment. In this work, a prototype *redundant sensor multi-gas detector* for carbon monoxide, oxygen and methane was designed, built, and tested. ***This prototype detector has significant improvements over conventional instruments due to the combination of redundant low power sensors and complementary dual detection technologies***. This approach enhances the reliability for detection of methane and carbon monoxide in a number of ways, such as improved accuracy, reduced baseline drift, and extended measurement range.

For detection of combustible gases, the prototype combines the broadly-accepted pellistor sensor technology with a chemiresistor. This approach will provide redundancy and reliable detection in a broad range of conditions. Both sensors were fabricated on Synkera's unique low power nanostructured ceramic microsensor platform. Pellistor technology is widely used in current portable gas detection instruments and some permanent gas detectors. Conventional pellistors are relatively small, affordable and offer a fast and accurate response to combustible gases. Unfortunately, the sensors are unable to reliably detect levels of methane above the lower explosive limit (LEL), or in oxygen deficient atmospheres, a significant problem for underground mines. Furthermore, these sensors are prone to poisoning, an effect which can only be partially mitigated by sensor design and operation, and have a power consumption that is excessive for use in a low-cost ultra-portable devices such as Synkera's Smart Gas Card™ design. In this project, we have built upon prior work and demonstrated the use of nanotechnology for an ultra-low power pellistor that is ideally suited for this application. Synkera has also pioneered the development of nanostructured chemiresistor sensors for detection of a wide range of combustible gases. *These chemiresistor sensors are capable of detecting elevated levels of flammable gases in the normal range of 0-100% LEL, as well as detection above the LEL concentration and in the presence of reduced oxygen, thus compensating for the shortcomings of the pellistor.*

For carbon monoxide (CO) detection, the electrochemical sensor is widely used in both permanent and portable applications. The sensors are generally recognized as relatively sensitive and selective. These sensors do not fail safe, prompting manufacturers to develop various schemes to interrogate the sensor, including bump testing, to ensure that the sensor is still functioning correctly. To address this issue and to enable the proposed redundancy, we combined a commercial off-the-shelf electrochemical sensor with a Synkera chemiresistor CO sensor. *The chemiresistor sensor provides insurance against an undetected failing CO sensor and reduces the effects of baseline drift upon the measurement.*

Translation of Findings

As described in Section 4 below, Synkera used advanced techniques involving nanomaterials, micromachining, and sensor fabrication to develop redundant sensors that are low power, miniaturized and affordable. After the prototype was built, methods and algorithms for combining the readings from the dual redundant sensors were explored and tested. This data fusion from two sensors results in a single, more reliable measurement for each target gas. Taken together, the

efforts in sensor fabrication, integration, and data fusion resulted in unique and significant improvements in the design of personal and permanent gas detection systems.

Currently, gas monitoring is accomplished via a combination of both fixed systems and portable instruments carried by workers. In recognition of the importance of personal gas detection for every individual exposed to hazards, new legislation was recently put into place [2] that in part requires mine operators to provide an "… MSHA-approved, handheld, multi-gas detector that can measure methane, oxygen and carbon monoxide to each group of underground miners". Better protection can be achieved if each employee is able to carry his/her own lightweight, affordable detector.

However, an additional barrier to be overcome is the unreliable performance of existing multi-gas detectors. *The number one concern universally expressed by users of safety instrumentation is reliability.* It is a well known truth in the sensor industry that there is simply no such thing as a perfect sensor, so safety instrumentation manufacturers attempt to match sensor features with applications as best as possible to maximize sensor performance and minimize chances for failure. Performance limitations that plague nearly all sensors in various ways and degrees include:

- Poor accuracy resulting in false positive or false negative readings
- Limited measurement range
- Significant baseline drift requiring frequent re-zeroing
- Susceptibility to environmental effects
- Poisoning or interference from other gases
- Lack of fail-safe mechanisms or warnings

As innovations in sensor technology and fabrication methods reduce sensor size and cost, it is now becoming possible to create hybrid sensor designs that employ two sensors capable of detecting the same gas using different technologies into one device. ***With appropriate choice of sensor types, good detector design, and the use of data fusion methods, redundant sensors can be used to eliminate or greatly reduce the impact of the performance limitations listed above.*** In this way, the overall system performance is dramatically improved.

Impact *(I)*

The potential outcome of the work performed in this program is a revolutionary new approach to alleviating intrinsic hazards of mining industry by equipping *every* miner with affordable and reliable personal safety tools. ***Synkera's approach addresses this opportunity by combining microsensors – pellistors, chemiresistors, and electrochemical sensors - into unique dual-element combustible and CO sensors to provide low power detection with extraordinary reliability.*** The technology developed here is suitable for integration with other commonly carried safety equipment and/or existing permanent gas detectors.

Future development of the technology developed herein will benefit from Synkera's ongoing relationships with some of the leaders in the gas detection industry (including Scott Health and Safety, MSA, Detector Electronics, Sperian (now owned by Honeywell), 3M, Net Safety Monitoring and others). We are currently seeking additional investment to develop the underlying technologies for full commercialization and product introduction in a variety of markets and applications, including industrial health and safety, indoor air quality, homeland security, and first-responders.

4. TECHNICAL REPORT

4.1 BACKGROUND

Nanostructured Anodic Aluminum Oxide for Microsensors *(I)*

Anodic aluminum oxide (AAO), produced from aluminum foil via an electrochemical process, is an anisotropic material with a high density of uniform and parallel nanopores, as shown in Figure 1. AAO pore diameter (5-300 nm), pore density (10^9-10^{11} cm^{-2}) and thickness (1-300 μm) are variable within wide ranges by controlling the conditions of anodization [3, 4]. In this project, the AAO morphology was fine-tuned in two steps. First, the *"primary porosity"* is defined during anodization. Second, "*secondary porosity*" is formed inside the primary pore walls as a result of annealing initially amorphous AAO into high surface area (80 m^2/g) polycrystalline alumina. *This approach yields highly reproducible sensing elements with a 10,000 fold increase in surface area relative to non-porous elements with similar dimensions. This enables high sensing volume per sensor footprint.*

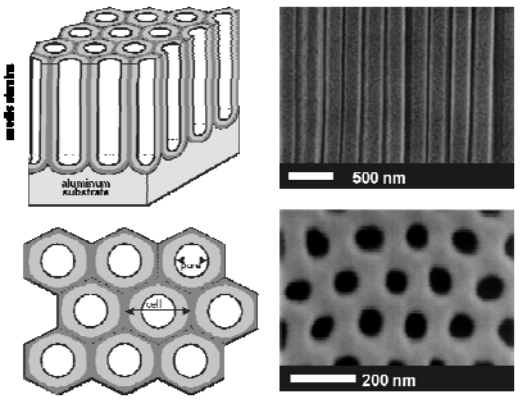

Figure 1. An "artist concept" and typical SEM images of AAO.

Synkera's approach to sensor fabrication (Figure 2) takes advantage of the unique properties of nanoporous self-organized Anodic Aluminum Oxide and Synkera's extensive capabilities in nano- and microfabrication with this material. AAO is an excellent material platform for gas sensing, including catalytic combustion (Figure 2), and represents a paradigm shift in sensor development and manufacturing. Synkera holds a key patent [5] on using this technology platform for gas sensors and other devices.

The nanoporous architecture and ultra-high surface area of AAO provide an ideal host for a well-dispersed and active catalyst, allowing uniform interaction of gas molecules with the catalyst dispersed though the sensing element, and thereby enabling high sensitivity. Additionally, AAO micromachining enables fabrication of thermally isolated monolithic microsensors with superior chemical, thermal and mechanical reliability. Temperature control is provided by a low power thin film microheater, which is deposited on one face of the sensing element and also serves as an integral resistive element temperature detector.

Synkera's technology for micromachining of nanoporous alumina ceramic provides a flexible and scalable design and manufacturing platform for realizing such dual element microsensors. To the best of our knowledge, there is no other ceramic micromachining technique with the same degree of versatility and manufacturability. It should be emphasized that sensors from polycrystalline alumina exhibit extremely high chemical, thermal, and mechanical stability, providing excellent prospects for high reliability in a wide range of environments. They can sustain continuous operation at up to 900°C, which is far beyond the reach of Si-based microsensors.

Pellistor-Type Combustible Gas Sensors

Combustible gases, including methane, are most commonly detected using either infrared (IR) or pellistor technology. IR detection is very reliable, but is most commonly used for permanent instrument applications, where the cost, power consumption and size of the detectors do not pose a problem for the users. Pellistor sensors are typically used in portable applications. In this case, the sensing of combustible gases is based on the change in sensor temperature due to the heat of combustion of gas molecules on a heated sensing element coated with a catalyst ("catalytic bead" or "pellistor", Figure 2). The sensing element is heated to a temperature at which it can catalyze oxidation of combustible gases:

$$C_xH_y,\ O_2 \rightarrow CO_2,\ H_2O + \Delta H;\quad \Delta H = f\,[C_xH_y] \sim \Delta T_{sens} \sim \Delta R_{heat}$$

The heat (ΔH) generated during combustion increases the sensor temperature as a function of the gas concentration, and the change in temperature is detected by the change in microheater resistance, thus providing usable measure of gas concentration.

The nanoporous architecture and ultra-high surface area of AAO provide an ideal host for a well-dispersed and active catalyst, allowing uniform interaction of gas molecules with the catalyst dispersed though the sensing element, and thereby enabling high sensitivity. Additionally, AAO micromachining enables fabrication of thermally isolated monolithic microsensors with superior chemical, thermal and mechanical reliability. Temperature control is provided by a low power thin film microheater, which is deposited on one face of the sensing element and also serves as an integral resistive element temperature detector.

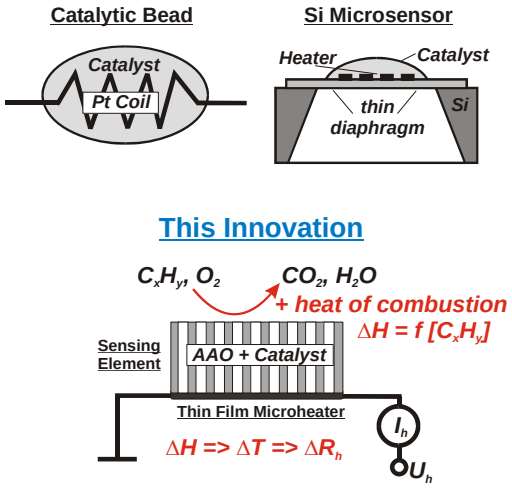

Figure 2. Synkera's innovative combustible gas sensor.

This is a fairly mature technology with numerous sensor products available on the market. However, miniaturizing this type of sensor to achieve low power consumption while maintaining performance and reliability has proven extremely challenging for the industry. Companies that manufacture combustible gas sensors include those that produce just sensors and those that produce sensors and detection instruments. The two largest companies in the first category are E2V Technologies [6] and City Technology [7] (a division of Honeywell), both of whom manufacture a wide array of "bead" type combustible gas sensors. Although both of these companies have sensors marketed for portable applications, their power consumption is in the 220-270 mW range, still too power hungry for truly small portable devices. Though not available for public offering, sensors manufactured by the instrument companies (e.g. MSA, Scott Health and Safety) are quite similar to those from E2V and City, with the lowest power at the ~250 mW level.

In addition, the reliability of all of these sensors is limited by concern over poisoning of the sensor response due to exposure to sulfur gases or silicones, which cannot be removed from the sensing surface during normal operation. Also the sensors require oxygen to provide an accurate reading, and do not operate reliably above the LEL. Efforts to reduce the effect of these challenges include the development of "poison tolerant" catalyst materials, and alarm locks that keep the instrument in alarm after an LEL exposure, to ensure that passing into an area with combustible gas above the LEL does not cause the alarm to end prematurely. Of course, this also makes it impossible for the user to detect if he/she has entered a clean area.

Electrochemical Carbon Monoxide Sensors *(I)*

Although several methods for the detection of carbon monoxide exist, amperometric sensors are the most popular option in many applications that require fast, accurate and selective sensors. These devices have a limited lifetime of approximately 1-2 years, and typically contain liquid electrolytes, which are prone to leak or dry out on long exposures to high or low humidity respectively which can interfere with their accuracy and significantly shorten their lifetime. Selectivity is attained through the use of a filter (usually activated carbon), which has limited capacity for scrubbing potentially interfering chemicals in dirty environments. In addition, the sensor response in the absence of carbon monoxide is a state of zero current output. Therefore the sensors do not "fail safe" as a lack of current due to a lack of CO present is indistinguishable from a lack of current due to a malfunctioning sensor. "Bump Checks" and sensor calibration are typically required to ensure the health of the sensors. The reliability of the CO measurement could be enhanced if the existing electrochemical sensors could be combined with an alternative technology that is rugged and long lasting, and guaranteed to fail safe. Synkera's chemiresistor sensors meet this need very nicely.

There exists an opportunity to substantially improve the state of the art sensing if a reliable sensor based on a solid polymer electrolyte could be developed. Commercial amperometric sensors use liquid electrolytes (often sulfuric acid), and are widely known in the sensor industry to suffer from electrolyte leaks under certain conditions. Indeed, the need to make electrical connections and allow gas into the sensor inevitably creates several opportunities for leak paths to develop. Additionally, because sulfuric acid is hygroscopic, the volume of the electrolyte changes with relative humidity, leading to changes in the sensitivity of the sensor response. The best solution to this problem is to use a solid electrolyte, an area that is being increasingly addressed in the literature. In previous work, Synkera has shown an ability to detect carbon monoxide, hydrogen sulfide and several organic species using our solid electrolyte sensors. In this work, we investigated the performance of several variations on nanocomposite solid polymer electrolytes (SPE) with our microband electrodes. The materials will be based upon polyethylene oxide (PEO) combined with appropriate inorganic salts (e.g. $LiClO_4$). These polymer electrolytes will be modified with nanostructured inorganic materials, such as alumina or titania, to form composites for optimum conductivity, stability and sensor performance [8]. Prior work at Synkera has shown that these electrolytes provide adequate ionic conductivity for sensor response at ambient temperatures.

Nanostructured Chemiresistor-type Sensors

Synkera's chemiresistor sensors utilize the same basic AAO microsensor platform described above, with the addition of a sensing electrode on the opposite face of the AAO substrate from the thin film platinum heater. Sensing materials (typically metal oxides such as tin oxide or zinc oxide) combined with catalytic promoters, are deposited into the pores using solution chemistries.

Metal oxide sensors undergo surface interactions (physisorption and chemisorption) with gas molecules at elevated temperatures (typically 200-400°C), resulting in a change in electrical resistance. As these materials are polycrystalline (i.e., composed of multiple grains with distinct grain boundaries), the adsorbed gases have significant electronic effects on the individual grains. These gas-solid interactions result in a change in electron (or hole) density at the surface (i.e., a space charge forms), which in turn changes the electrical conductivity of the oxide. An example is the interaction of SnO_2 or TiO_2 with molecular oxygen. O_2 chemisorbs on these materials, producing negatively charged oxygen ions, O^- and O_2^-, via removal of electrons from the conduction band of the metal oxide. Thus, there are fewer electrons in the surface space-charge region, and the overall conductivity decreases. A similar reaction occurs when reducing gases, such as H_2, interact with semiconductor surfaces, resulting in adsorbed positive ions, H^+ on the surface and a corresponding increase in conductivity.

Recent work in chemiresistive sensing has been in the area of thin vs. thick film sensors (produced by either spin or dip coating from wet chemical solutions) and nanoengineered grain structures.

Several researchers [9,10,11] have reported a substantial performance increase in metal oxide sensors as grain size is reduced to the "nano" level. Synkera has utilized this "nano" effect, in conjunction with advances in materials chemistry and our novel microheater platform, to produce a commercially superior solid-state sensor technology for the detection of several important toxic gases.

4.2 SENSOR FABRICATION AND CHARACTERIZATION

During this project, Synkera worked on advancements in our SPE electrochemical , pellistor and chemiresistor sensor technology described above to support fabrication of the redundant sensor prototype. Details are provided in the following sections.

4.2.1 Electrochemical CO Sensor

Synkera considered the use of a novel SPE based electrochemical sensor for inclusion in the prototype detector, building on prior work completed in the sensing of ozone [12], and hydrogen sulfide [13]. Two basic designs were considered: a planar structure and a multi-laminate structure with microband electrodes. Ultimately, we chose to use a commercially available sulfuric acid based electrochemical sensor in order to overcome problems with humidity response in the CO sensor developed for this project. With additional effort, it might be possible to create a sensitive and selective CO sensor using the Synkera SPE design.

Sensor Assembly *(I)*

The solid polymer electrolyte (SPE) used for both the microband sensors and the planar electrodes were prepared via solution techniques. Two methods were utilized, 1) direct solution deposition onto the electrode substrate, and 2) casting of films from solution followed by the application of the films to the electrode. For both processes electrolyte solutions were prepared. Desired ratios of polyethylene oxide (PEO) and an electrolyte salt (e.g. LiCl, $LiClO_4$) were dissolved in a mixture of methanol and toluene. In some cases modifiers such as surfactants and ceramics were added to the solution. Once a solution was prepared it was ready for direct solution deposition, or to be cast into thin polymeric tape. Tape casting was performed by spreading the solution between two 0.020" shims and allowing it to dry. Once dry the tape was pressed at high pressure (10,000 lbs.) to further thin the tape and press out pin holes. Thin tape (electrolyte film) is required to allow analyte diffusion to the working electrode.

The planar electrodes were prepared with both the working and the counter/reference electrodes screen printed onto an alumina substrate (Figure 3, Left), and the electrolyte was simply applied over the top of both electrodes, leaving a small portion of each electrode uncovered to allow for electrical contact to be made. For solution deposition, a coating of the electrolyte solution was placed on the electrodes and allowed to dry at room temperature. Multiple applications were performed to achieve the desired film thickness. For the application of the thin tapes, the tape as pressed was cut to the appropriate size; one side of the tape was wetted using water and then applied to the electroded substrate. The tape was firmly pressed to the substrate to ensure adhesion and then allowed to cure in room air. An example of a planar sensor with enhanced Pt working electrode and PEO/LiCl tape electrolyte is shown in Figure 3, Left.

Sensors were also built using a multi-laminate process. This novel architecture allows for the production of low-cost, highly reproducible sensors that take advantage of the features of microelectrodes. In this case, the thin sheets of polymer electrolyte are used as the support material between the electrodes Gold and platinum electrodes are printed on some of the sheets, and then a "pad" is built via the successive lamination of individual sheets. Sensor preparation is completed by dicing the pad into individual components to expose the working electrode edges, while the counter/reference electrodes are buried within the SPE body. A sketch of the sensor

(I) Invention Data,-Synkera Technologies, Longmont, CO

design, and a selection of sensors fabricated via the multi-laminate process are shown in Figure 3, Center and Right.

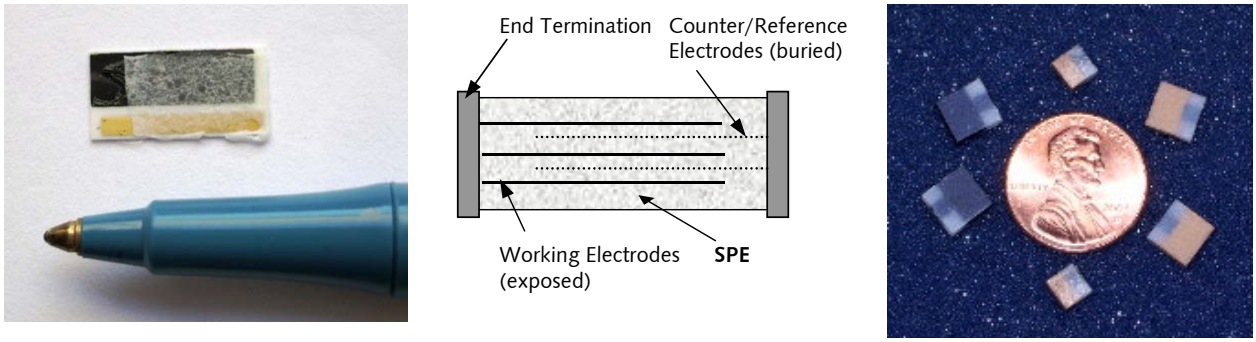

Figure 3: Two configurations used for SPE electrochemical sensor fabrication: (Left) planar, (Center) a sketch of the microband electrode concept and (Right) multi-laminate sensors with exposed microband electrodes

Sensor Evaluation

Over 150 variations in sensor geometry, electrolyte composition and bias voltage were explored. Sensors were tested with carbon monoxide concentrations of <50 to 1000 ppm) as they were produced and additional testing (repeatability, stability, selectivity, humidity) was performed on the best performing sensors. Bias voltages from -500 to 500 mV were explored. Over 150 variations in sensor geometry, electrolyte composition and bias voltage were explored. While most of the compositions did respond to CO, none of the responses (taking into account sensitivity, selectivity, linearity, repeatability, response time and stability), were considered good enough for use in the prototype detector. The biggest problems were stability over time and a problematic false response to water vapor.

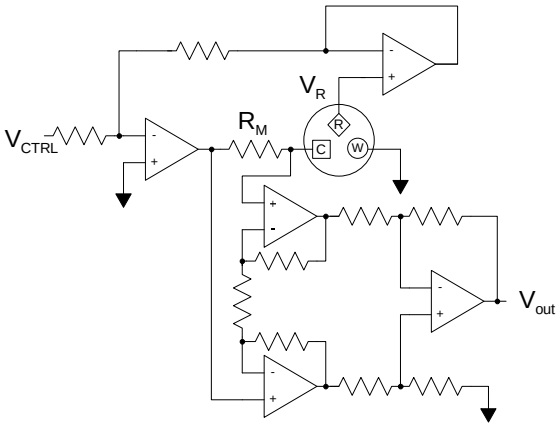

Figure 4: Potentiostatic control circuit

Initial testing of the electrochemical sensors was performed using an in-house potentiostat (Solartron 1260). More extensive testing was performed with a simple but effective control circuit previously designed and implemented at Synkera. The circuit is based on the classic potentiometric control circuit shown in Figure 4. For the solid-state electrochemical sensors being developed, the voltage at V_{CTRL} works in conjunction with the reference electrode R to keep a fixed potential between the counter electrode C and the working electrode W.

V_{out} is proportional to the current through the cell, and can be ranged via selection of R_M. This circuit has been previously implemented at Synkera in a two-electrode fixed potential solid-state sensor transducer. Because this circuit was designed specifically to operate Synkera's solid-state electrochemical sensors it is be stable and reliable for current measurements as low as 50 pA, making it more suitable than commercial potentiostats designed for a much wider range of measurements.

4.2.2 Chemiresistor CO / CH_4 Sensor

This project relied on Synkera's Ceramic MEMS technology based on AAO (described above, [14, 15]) for creating low power chemiresistor microsensor substrates.

Sensor Assembly *(I)*

During this project, Synkera fabricated chemiresistive ceramic MEMS sensors using the processing techniques of hybrid ceramic micromachining, localized anodization and anisotropic etching. The basic processing sequence for fabricating Ceramic MEMS devices from nanoporous anodic aluminum oxide includes the following steps:

1. Prepare Al foil of required thickness and temper by cold rolling and pressure-annealing from stock Al foil (this step now being outsourced for efficiency)
2. Anodize aluminum to form porous AAO of required thickness and morphology
3. Micromachine AAO using localized anodization and optical contact lithography to define sensor substrates of desired design
4. Anneal produced sensor substrates to required phase composition
5. Deposit functional metal electrodes
6. Deposit sensing materials via screen printing or solution
7. Package sensor platform

The chemiresistor sensor substrates for this effort were 50 μm thickness with 35 nm pores, which provides a good balance of low mass (for low power consumption), strength and mechanical integrity, and good sensor response. Sensing materials were deposited using both screen printing (to allow deposition of a uniform film of material on the surface of the microheater substrate, and solution, to allow penetration of sensing materials into the high aspect ratio nanopores.

Sensor Evaluation

Heater control is an important consideration since most chemiresistor sensors need to be operated at an elevated temperature. The optimum operating temperature is dependent on the sensing material of choice and the gas(es) to be detected. The required heater input (voltage, current, power) is dependent on sensor construction and target analyte.

The chemiresistor CO and CH_4 sensors are n-type, which means that when exposed to target gas, the resistance of the sensor decreases. For the N-type circuit (Figure 5), the transfer function is ***Vout=Vbias*(1 + Rf/Rsen)***.

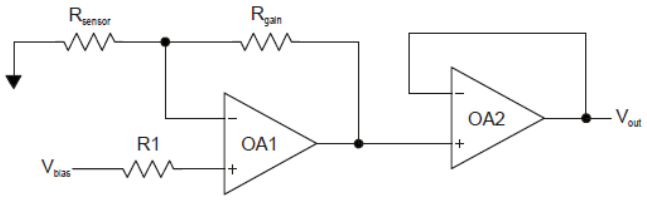

Figure 5. Simplified n-type circuit

The advantage of Synkera' n-type circuits are that they work with large values of sensor resistance and large responses to analytes (up to a few orders magnitude) due to the approximate log relationship transfer function and low leakage current of the OPAMPs. This combined sensor/circuit behavior also serves to minimize baseline drift.

Dozens of sensors of varying compositions were made to explore their suitability for use in this project. Tests included sensitivity, selectivity, repeatability, stability response time and linearity. The sensors were tested at a range of heater voltage inputs from 160 mW to 270 mW. The applied heater power (related to operating temperature) can be used to tune the selectivity of the sensors to varying analytes.

A typical linearity plot is shown in Figure 6. In this case, a single sensor is operated at a power input (230 mW) that will allow it to respond to both carbon monoxide and methane. The sensor is tested with carbon monoxide, methane and propane. The propane is used as an indication that the sensor is not specific to methane, but rather reacts broadly to flammable gases as a category. The concentrations tested, expressed in ppm, are selected to be relevant to alarm levels. The LEL of methane is 5%, or 50,000 ppm; alarms are typically set at 10% or 20% LEL. The LEL of propane is 2.1% by volume.

Sensor resistance is plotted versus applied concentration of analyte, and a log scale is used due to the large ranges covered. As expected, the sensors show a significant, repeatable decrease in resistance on exposure to analyte.

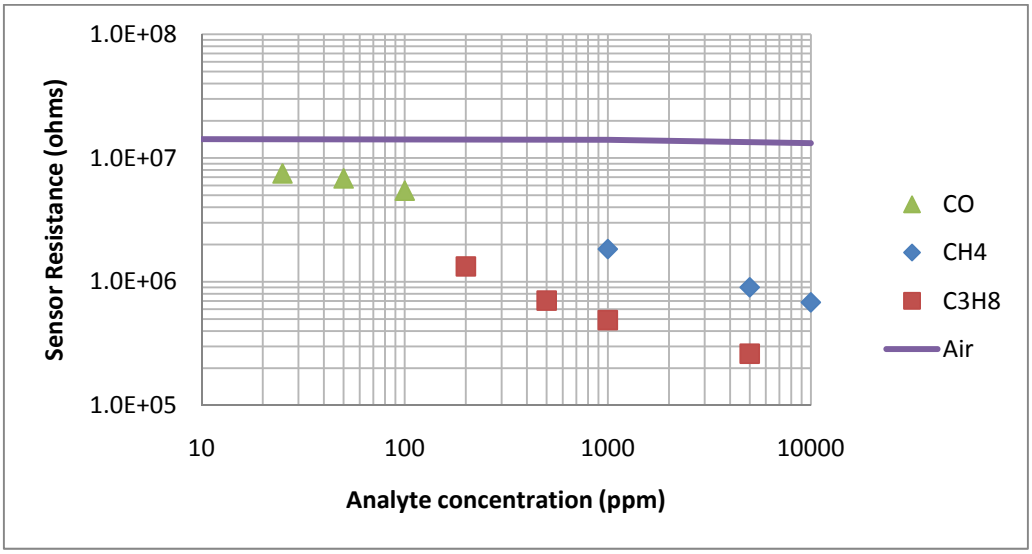

Figure 6: Response of chemiresistor sensor to carbon monoxide, methane and propane.

A typical response curve is shown in Figure 7, for three sensors of a single design, each operated at 230 mW. Here, the resistance of the sensors as a function of time is plotted as the concentration of methane is changed. This plot demonstrates the fast response and recovery, and is an illustration of the type of data that was taken throughout the project in order to characterize the sensors.

Additional data is available upon request.

4.2.3 Pellistor Sensor (CH_4)

The focus of the pellistor sensor effort within this project was the characterization of Synkera's prototype pellistor sensors developed under NIOSH SBIR funding [16].

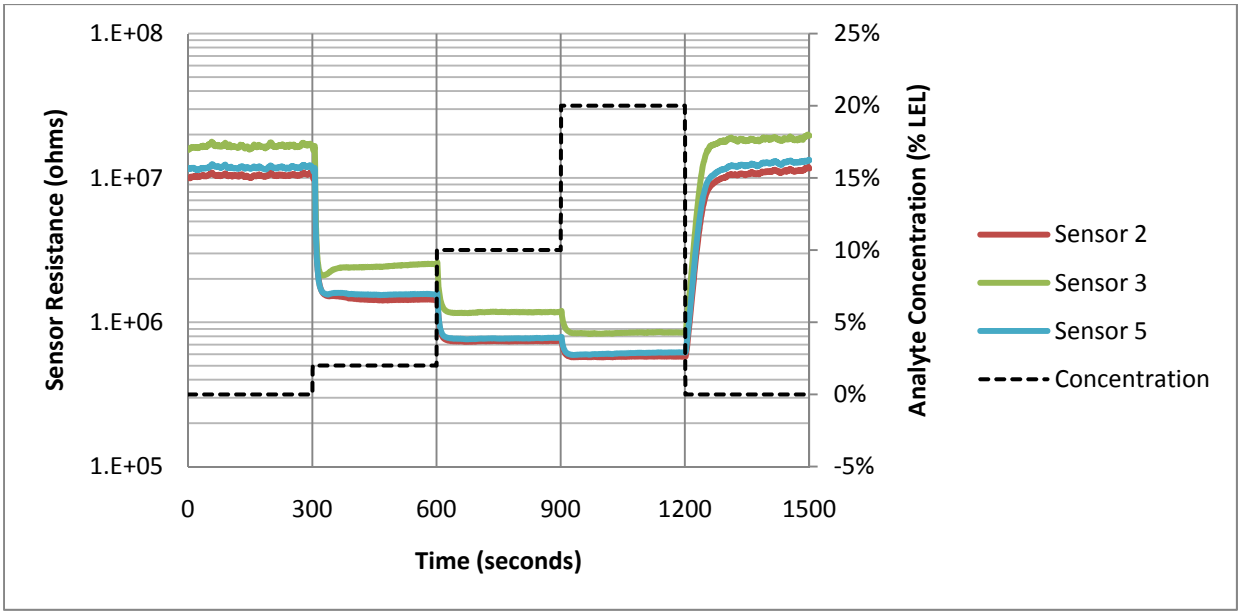

Figure 7: Sensor response to changing methane concentration as a function of time

Sensor Assembly

Sensors were fabricated for this project following the Phase I design and procedure. The pellistor sensors use the same basic micromachined ceramic as the chemiresistor sensors, but with a dual element design to allow for use of an active and reference element in a bridge circuit (the classic pellistor design). The unique feature offered by Synkera is the low power, reliable performance enabled by the high surface area micromachined anodic alumina substrate. Deposition of catalysts inside the pores and onto the surface of AAO enables catalytic oxidation of combustible gases at the active element. In this work, generic Pd/Pt catalysts were used with metal oxide promoters [17], such as colloidal alumina, to increase catalyst performance. Wet chemistry methods work well for deposition in very high aspect ratio (length/diameter) pores, yielding good sensor performance.

Images of a prepared, packaged sensor are shown in Figure 10.

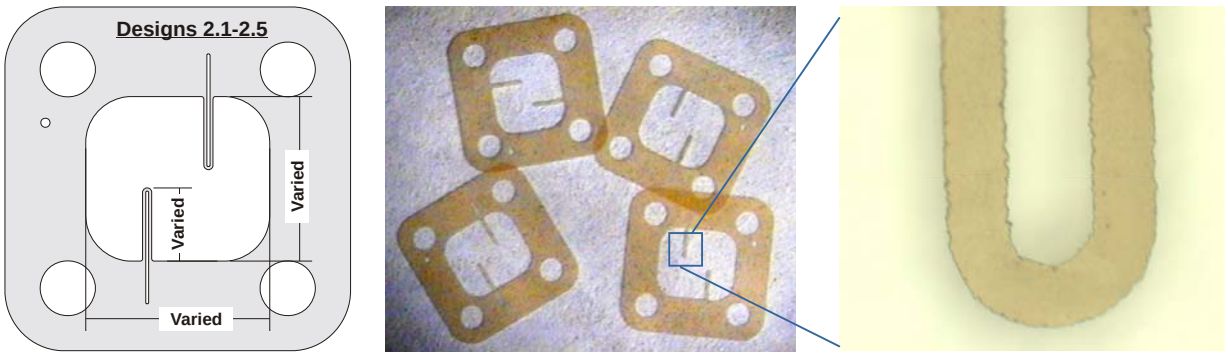

Figure 8: (Left) Pellistor sensor design and (Center, Right) Examples of blank low power microsensor substrates

Sensor Evaluation

Virtually all commercial pellistor-based sensing systems use bridge-based ratiometric circuits for measurement of the resistance change that occurs in the active pellistor element when combustible gas is present. A bridge circuit that could support both a constant voltage and constant-current mode of operation was previously built in used in sensor characterization and the prototype RS-MG unit (Figure 9). The bridge balance voltage is amplified with adjustable gain (G=18 to 50) to handle variations in sensitivity. The applied voltage, current draw, and bridge output signals are available on an external connector for interfacing to a data acquisition system.

Figure 9. Combustible gas sensor support circuit (2"x3" SMT PCB).

Figure 11 shows the response of three pellistors as a function of time. As the bridge output is recorded, the methane concentration is changed from 0% to 5%, 10%, 20% and 50% LEL (up to 2.5% by volume). As with the chemiresistor data, this plot is typical of the way data was taken to characterize the sensors. Again we see a fast response and recovery time. The sensor response is linear with respect to concentration.

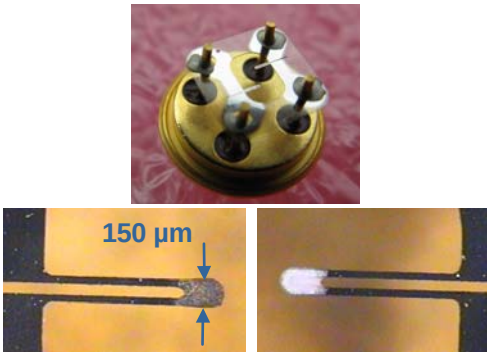

Figure 10. Prototype of the low power sensor and close up of the sensing and reference elements.

Next, we show the repeatability of three pellistor sensors (Figure 12) when exposed to repeated step concentrations of 0, 30% LEL (1.5% volume), 42% LEL (2.1% volume) and back to 0%.

The sensor response is repeatable, and shows no degradation over this short period of time. More extensive tests were run, but are not shown here. More data is available upon request.

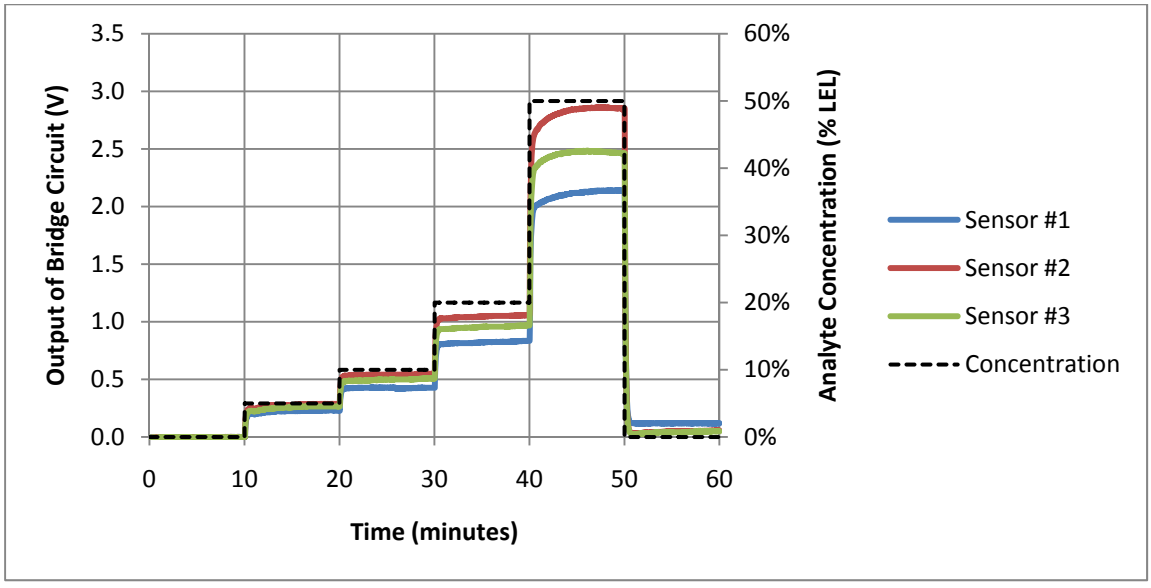

Figure 11: Response of three pellistor sensors to changing methane concentrations as a function of time

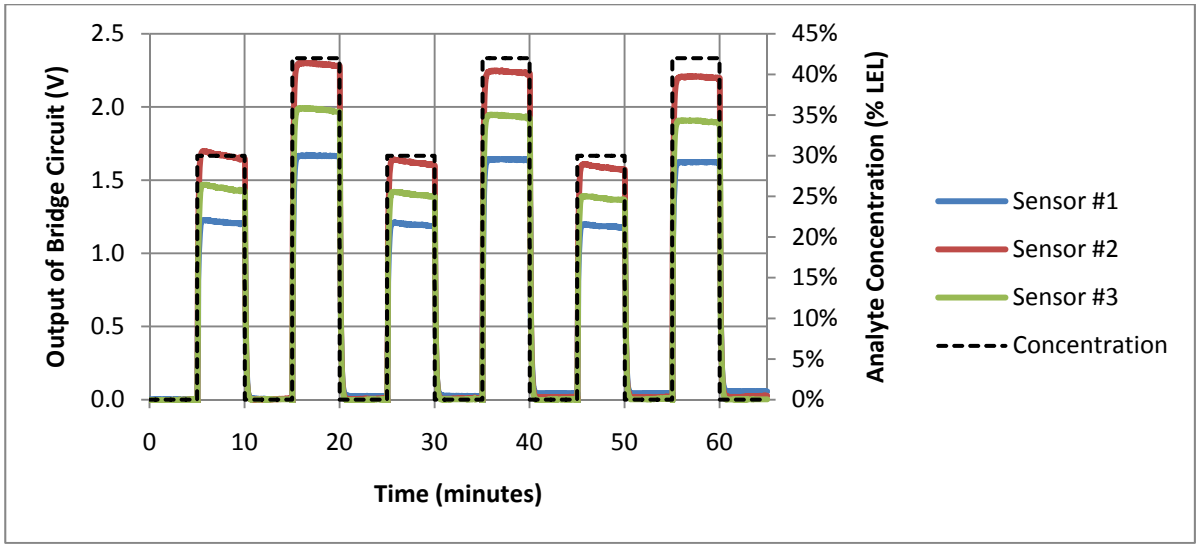

Figure 12: Repeatability of three pellistor sensors to changing methane concentrations

4.3 REDUNDANT SENSOR MULTI-GAS DETECTOR PROTOTYPE CONSTRUCTION

Description of Sensors Used

For mine safety applications, there are 3 gas types that are usually monitored: oxygen, combustibles (often CH_4), and toxics (H_2S and/or CO). For this project, it was proposed that we would focus on the construction of a 3-gas detector to monitor O_2, CH_4, and CO. A brief description of the sensors used in the construction and testing of the prototype is given below.

For the O_2 sensor, a miniature echem sensor from Alphasense (Model #O2-A2) was used. This sensor has good linearity and excellent performance in a reasonably compact miniature package. For combustible detection, two Synkera-developed sensors were used as described in the previous sections: a 4-electrode MOS microsensor and a dual element micro-CGS sensor. For CO detection, a miniature commercial electrochemical sensor from Alphasense (CO-D4) was paired with another Synkera 4-electrode MOS microsensor. The range and key performance traits of the commercial sensors used above are comparable to that found in commercially available multi-gas detectors, such as the GasAlertQuattro from BW Technologies or the Altair4X from MSA. A total of five sensors is thus used in the 3-gas RS-MG detector prototype.

Hardware Developed

Each of the five sensors requires a preamplification/signal conditioning circuit. In previous projects, Synkera has developed suitable circuit designs compatible with each of these sensors. The CGS circuit is based on a Wheatstone bridge, while the chemiresistor and electrochemical sensors utilize a current-to-voltage converter design. These circuits also provide for microheater control. In this project, these 5 boards were integrated with an analog to digital controller (ADC),

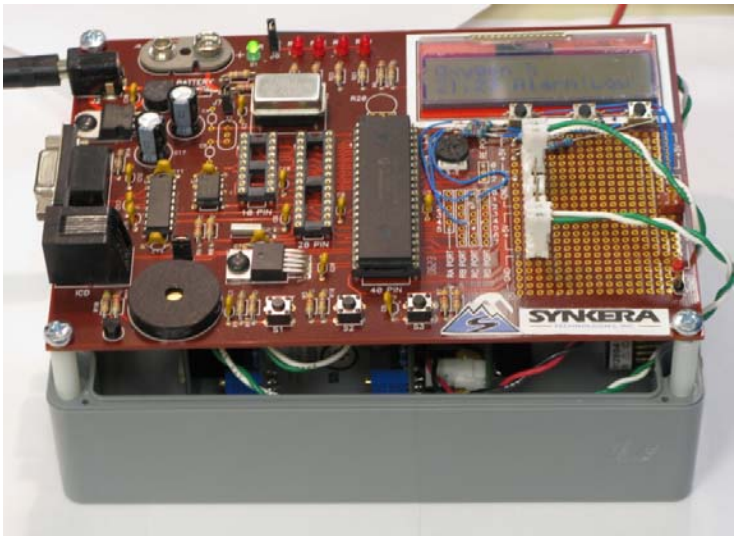

Figure 13. Prototype redundant sensor multi-gas detector for mine safety constructed during this project.

microcontroller, LCD display, and EEPROM chip to allow for datalogging and user control over detector functions. The boards were assembled onto a frame and placed into a 6.5″ x 4.5″ x 1.5″ polycarbonate enclosure, as shown in Figure 15.

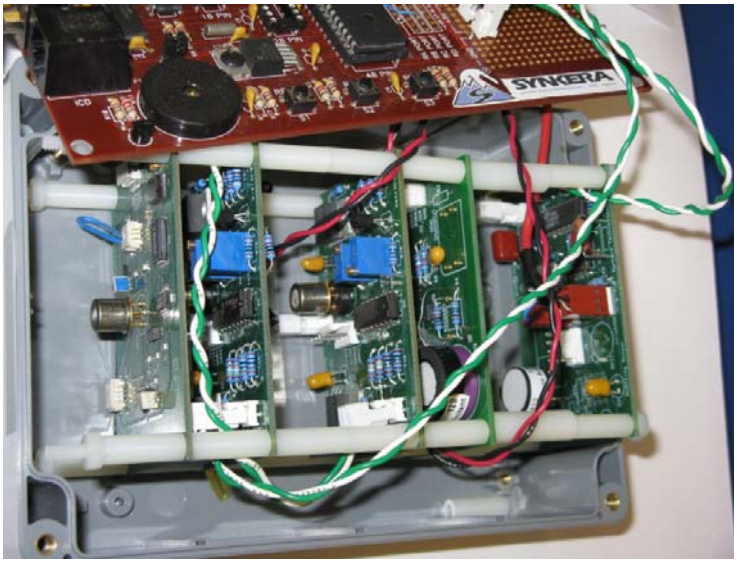

Figure 15. Five sensor boards used in the RS-MG prototype. Microsensors in TO-39 packages and echem cells are mounted on the individual boards.

The overall design is based on a Microchip PICDEM2 Plus evaluation board with a PIC18F452 microcontroller. All sensor boards were modular to allow evaluation of multiple types of sensor signal conditioning circuits. This design allows us to adopt any virtually any kind of sensor or sensor circuits for use in the prototype, so long the final sensor output is a 0~5V analog signal. In the final project-specific implementation we have total 5 analog channels, and they are: 1) Electrochemical CO sensor, 2) Oxygen fuel cell sensor, 3) Solid state chemiresistor combustible sensor, 4) Pellistor combustible sensor, 5) Solid state chemiresistor CO sensor. Also included is a digital temperature sensor. Figure 13 shows a photograph of the assembled prototype RS-MG unit. A block diagram of the prototype constructed during this project is shown in Figure 14. This modular design also gives us the flexibility of expanding the instrument to include more gases to be detected in future development efforts.

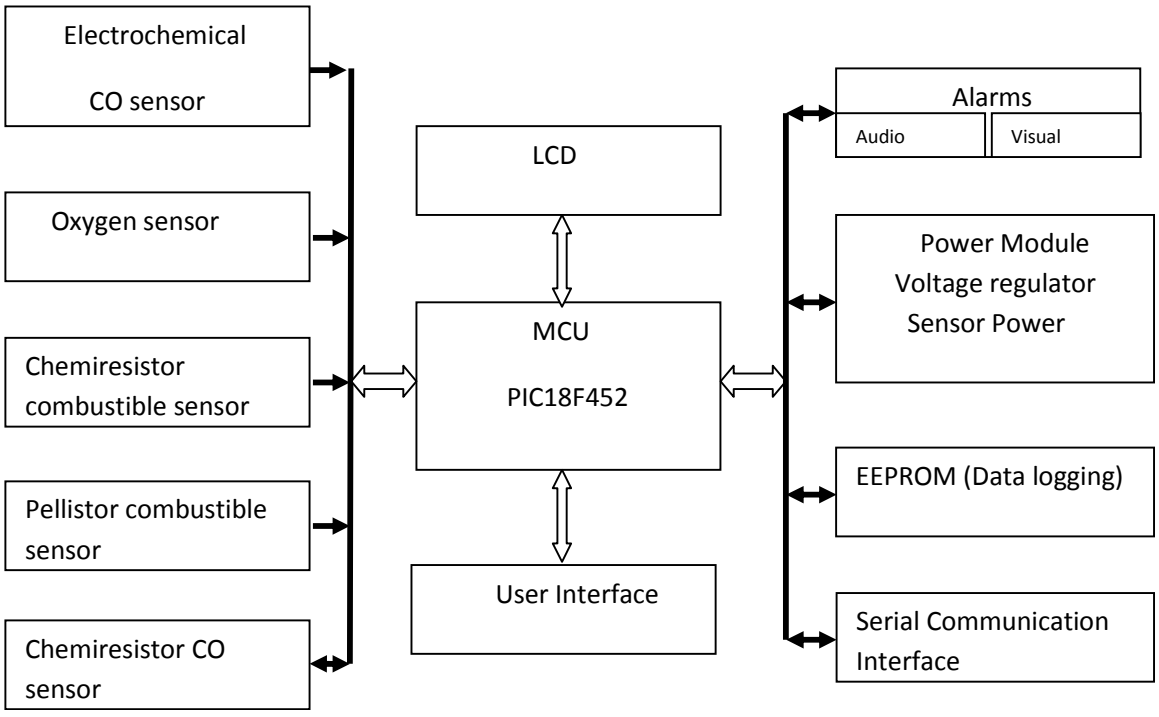

Figure 14. System block diagram of the prototype RS-MG detector.

Firmware/User Interface

The firmware design includes data acquisition module, communication module, menu operation module, data processing and display module and alarm module. A flexible display mechanism is also designed to display all gas concentrations (by cycling all possible channels), or a certain fixed channel can be selected for display. Display options are conveniently configured through the user interface or serial commands from a computer. Several photos showing the RS-MG unit under various gas conditions are shown in Figure 16.

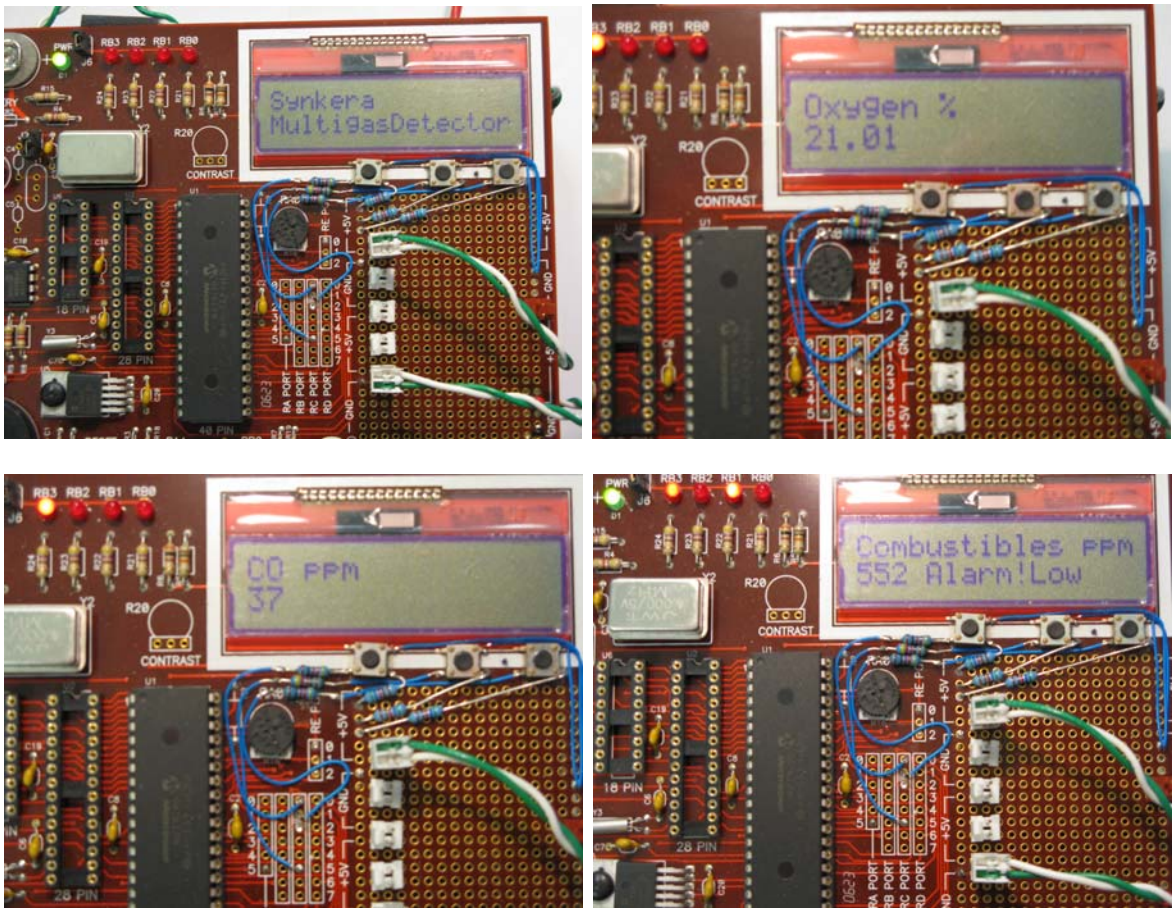

Figure 16. Prototype RS-MG detector under exposure to various gas conditions.

A concise six button navigation type user interface has been implemented in the instrument design. It only consists four directional arrow keys, an enter key, and a reset key. Various menu operations are available, such as time and date settings, alarms setting and calibration operations. Visual alarms were implemented via the use of red LEDs and audio alarms are possible via a buzzer.
A menu tree structure outlining the various user functions is shown in Figure 17.

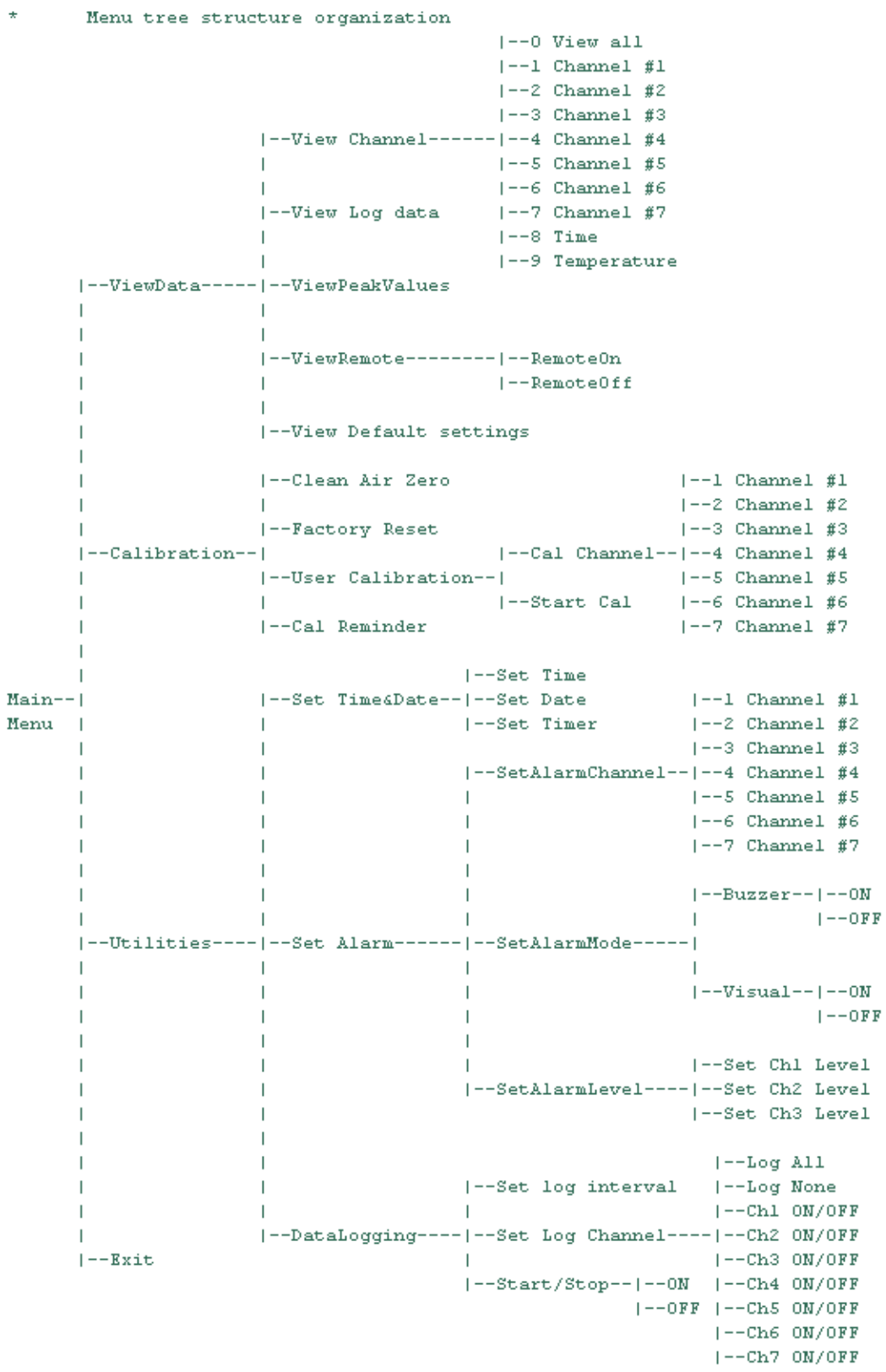

Figure 17. Menu tree structure of user commands for the RS-MG detector prototype *(I)*.

4.4 REDUNDANT SENSOR TESTS AND DATA FUSION

Key Operating Parameters

During the work described in Section 4.2 above, Synkera fabricated chemiresistors and pellistors that deliver good overall performance, due to optimized sensing materials, nanostructured platform, and determination of best operating parameters. Sensors from this group were selected and loaded onto their respective PCBs. In preparation for sensor calibration and redundant sensor validation testing, key operating parameters were determined and set for each sensor as described in further detail below.

One very important parameter that governs pellistor performance is how closely matched the resistances are for each element. Experience has shown sensors with matched resistances for each element give the best response stability and linearity. After selection of a CGS sensor with suitably matched elements, the next step is determination of heater voltage. The plateau region on the IV curve gives the most stable response and greatest difference in the response in air versus combustible gas and allows determination of a suitable operating power (heater voltage).

For the chemiresistors, the heater bias voltage is set to achieve the desired operating temperature (power) that works best for the combination of sensing material and target gas. Next, sensor resistance in air and challenge gas is measured. These values are then used to determine what gain resistor should be used in the pre-amp circuit to ensure that the sensor response within the range of interest falls within the range of the ADC. Gain and offset adjustments were made via potentiometers to fine-tune the response range. For maximum stability, the sensors are left on power for a period of 24 hours prior to calibration, to allow for sensor conditioning and burn-in, a common procedure for chemiresistors. In field portable operation, this burn step can be eliminated through the use of heater stabilization pulses.

Sensor Calibrations

For sensor calibration and redundant sensor validation testing, a custom-built gas test system was used. This test system utilizes calibrated mass flow controllers, custom electronics, and a LabView interface for control and data acquisition. Gas sources are certified standard grade from Airgas. For CH_4 testing, a cylinder containing 2.5% CH_4 in air was used, while for CO testing, a cylinder containing 750 ppm CO in air was used. Blending of the gas standards to produce desired setpoint concentrations was accomplished using mass flow controllers (MKS 1179A), which are calibrated versus a digital glass bubble meter with a NIST-traceable calibration good to 0.3% relative accuracy.

Calibration data sets were recorded over the intended validation range for all sensors to be tested, as shown in Figure 18a, below. For CH_4, this range was 0-25,000 ppm and for CO, this range was 0-300 ppm. Calibration data was plotted and appropriate best fits to the data were performed to determine calibration coefficients. An example of the fitting process for one sensor is shown in Figure 18b.

For the chemiresistors, log-log relationships between response and concentration were used to fit the data, while the CGS and electrochemical sensors were found to have linear relationships, as expected. Lastly, calibration equations and coefficients were entered into the firmware code and programmed into the multi-gas detector microcontroller. These procedures are equivalent to the factory calibrations performed by competitive instrument manufacturers.

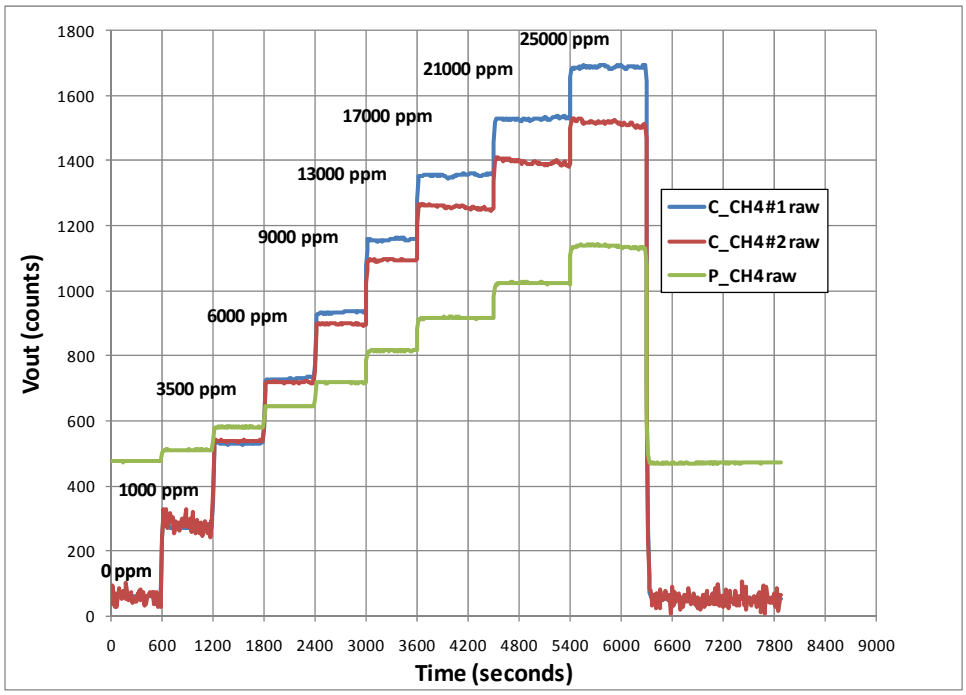

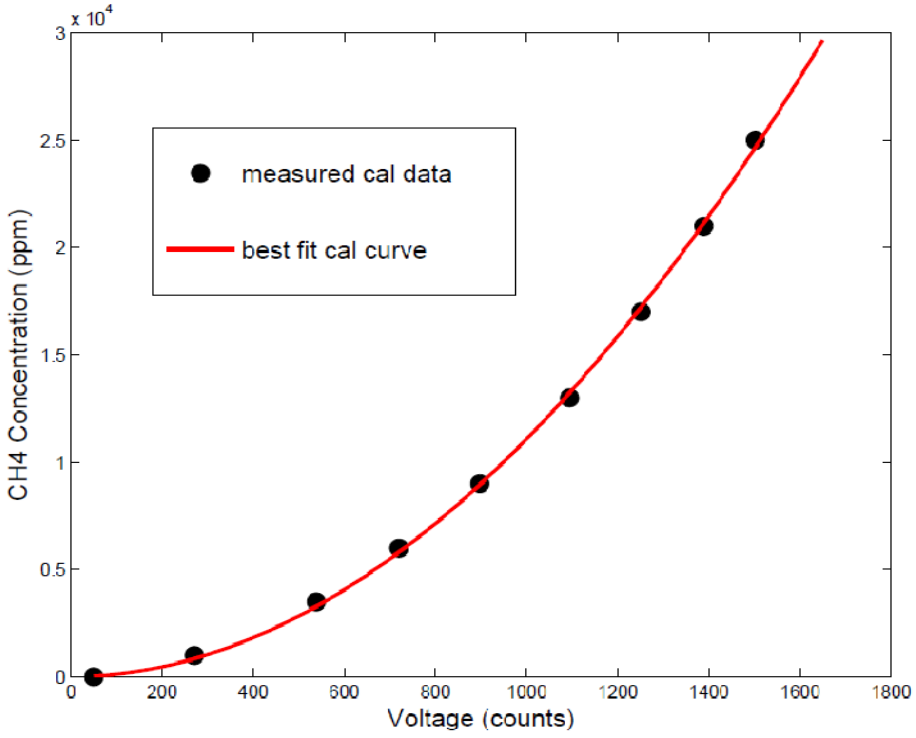

Figure 18. Calibration of redundant CH_4 sensors.

Redundant Sensor Testing *(I)*

After sensor calibration was complete, our attention turned to side-by-side testing of the redundant sensors for CH_4 and CO. For these tests, two MOS microsensors were chosen having the same composition (eg. SnO_2 for CH_4) but from different production batches. Two MOS sensors were used, rather than a single sensor, because MOS sensors can have considerable variation in behavior, even among sensors that were produced in the same manner. These two MOS sensors were tested side-by-side in the prototype RS-MG detector with the appropriate complementary sensor for the target gas (Synkera CGS sensor for CH_4 or Alphasense echem sensor for CO). *Sensors were tested in the RS-MG detector, because sensor performance is not only governed by the sensor itself, but is also influenced by the pre-amp circuit and system electronics used to convert raw sensor output to calibrated readings*. The experiments described below had several goals:

- Evaluation of accuracy and overall performance for each sensor within the RS-MG unit
- Collection of a database of responses from individual sensors to be used in developing data fusion algorithms
- Evaluation of the data fusion algorithms (primarily in terms of accuracy) via post-processing of the datasets

The work performed toward each of these goals is described in further detail below.

When tests were run, a plastic test head was placed over the packaged sensors (having openings appropriately sized for the TO-39 package or the miniature size echem cell) to introduce the same gas stream to each sensor via use of upstream tee's. The sensors were exposed to a single challenge gas, CH_4 or CO, over a series of gas concentrations falling within the calibrated range for the sensors. Validation concentration setpoints were were different from the calibration setpoints. The total gas flow rate used was 500 mL/min, split evenly amongst the various sensors. A series of five side-by-side tests were performed, one per day for each gas. Typical results obtained for a methane test are shown in Figure 19. A Matlab script was used to process the concentration time series data, (Figure 19a), by averaging the final 90 seconds of data at each concentration step for each sensor. These measured readings can then be plotted versus the expected reading at each setpoint (Figure 19b). Data for CO tests was processed in the same fashion.

A more informative method to visualize the test results is to utilize error plots, which show accuracy relative to a specified error budget. Absolute errors (measured value – expected value) were calculated and then plotted versus expected value. Results obtained for all methane tests are shown in Figure 20 on the following pages. MSHA document STP 2203, entitled Methane Detector Accuracy Test, gives maximum allowable absolute errors for portable instruments measuring methane in air at specified concentrations ranging from 0-50,000 ppm. For CO instruments, ISA document S92.02.01 gives error limits for CO for portable and stationary instruments for measuring CO. These limits are shown in the respective figures below.

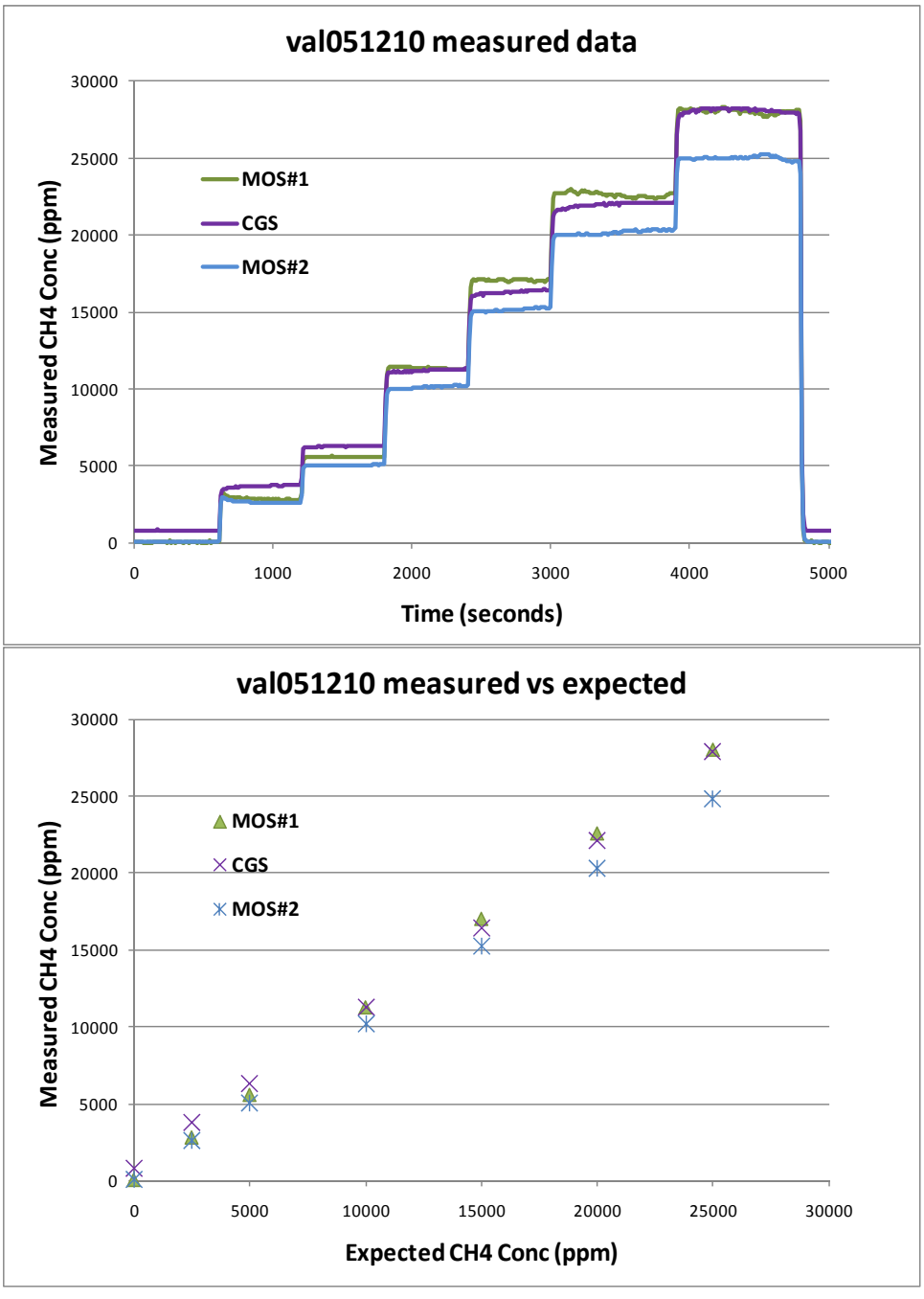

Figure 19. Typical redundant sensor validation test results.

A number of interesting features were observed in the CH_4 data. First, the two MOS sensors were fairly consistent, with errors that tracked each other fairly well. Turning to the CGS sensor, the errors were remarkably consistent from day-to-day indicating the presence of a systematic error. The source of this error is unknown. Lastly, the CGS sensor had considerable offset error (variation in zero reading) that varied in a random fashion from day-to-day. The MOS sensors did not have this variation in zero reading. This behavior for the CGS sensor is likely due to the highly Wheatstone bridge circuit used for preamplification. This circuit is extremely sensitive to any differences in resistance between the two elements on the sensor and thus appears to be more susceptible to noise or other random error sources that affect the two elements differently. Since these offset errors resulted in the CGS sensor being out of budget for 4 out of 5 datasets, a zero correction was post-processed and is also shown in the plots. This may point to the need for frequent re-zeroing of the CGS microsensor and has ramifications for the data fusion algorithms, as discussed further in the following section.

For CO instruments, ISA document S92.02.01 gives error limits for CO for portable and stationary instruments for measuring CO. Turning to the CO data, shown in Figure 21 and Figure 22 below, we can see that the MOS and echem sensors had similar overall performance relative to the error budget, with the echem sensor tending to have somewhat more consistent errors than the MOS sensors. Unlike the CGS sensor, the echem sensor had a relatively stable zero reading. Examination of the CO calibration data shown in Figure 21, shows another key difference between the MOS and echem sensors for CO. Redundant CO sensor calibration data showed response saturation at concentrations > 300 ppm for the MOS sensors. MOS sensors are known to exhibit fall-off at higher concentrations in some cases due to exothermic surface reactions. The echem sensor does not have this range limitation, demonstrating another benefit of the redundant sensor approach. Redundant sensors could be used, in this case, to extend the CO measurement range to higher concentrations than those possible with a single sensor type.

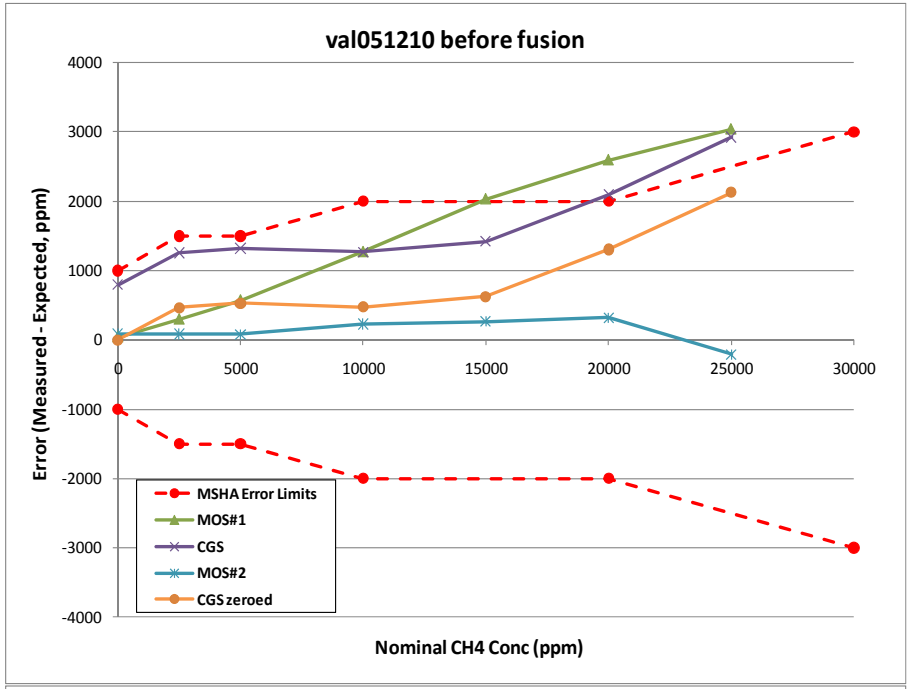

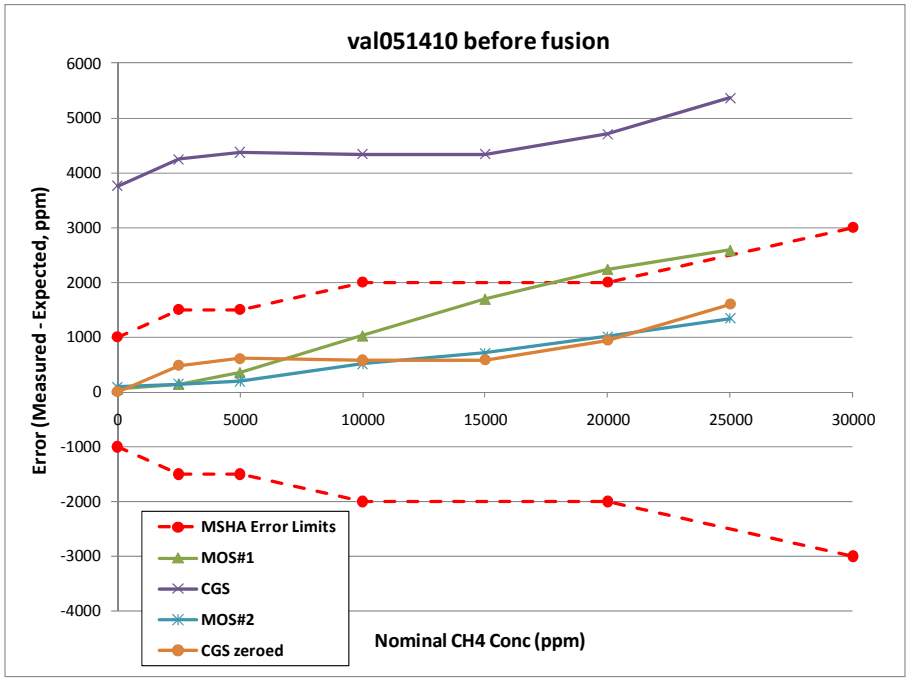

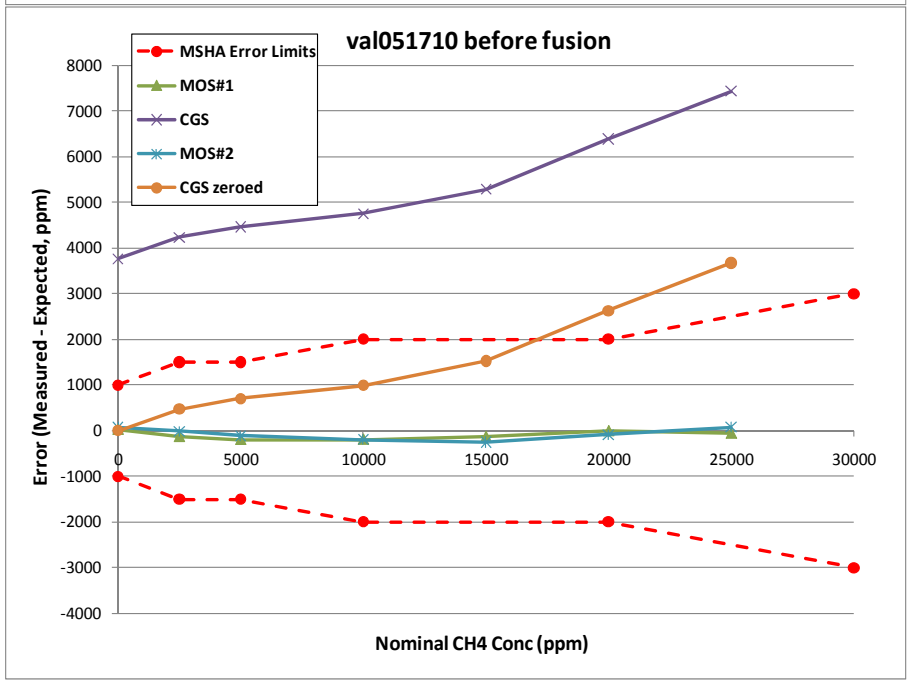

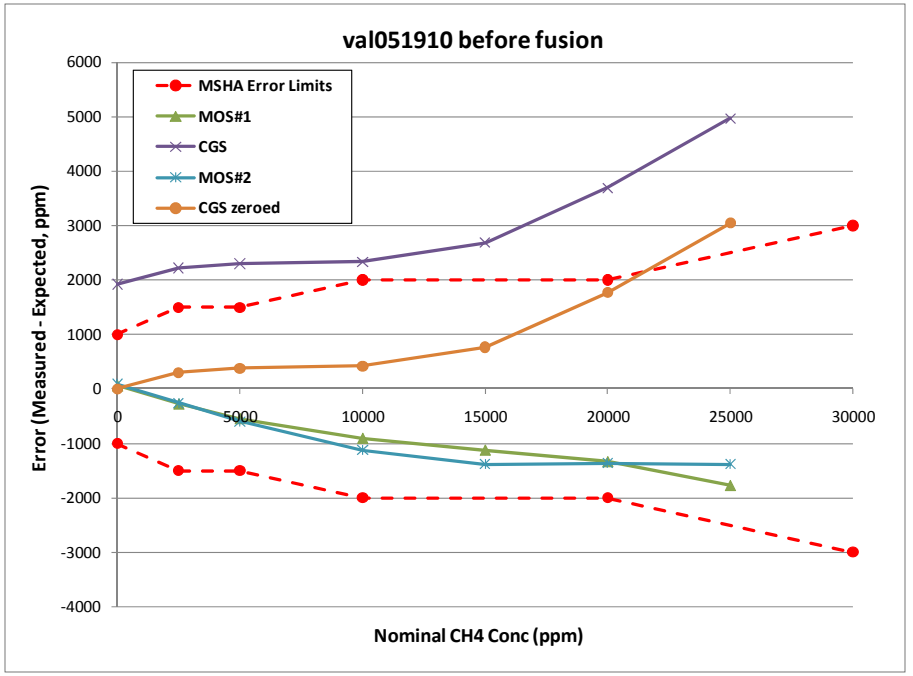

Figure 20a-d. Errors vs. budget for individual redundant CH_4 sensors before data fusion.

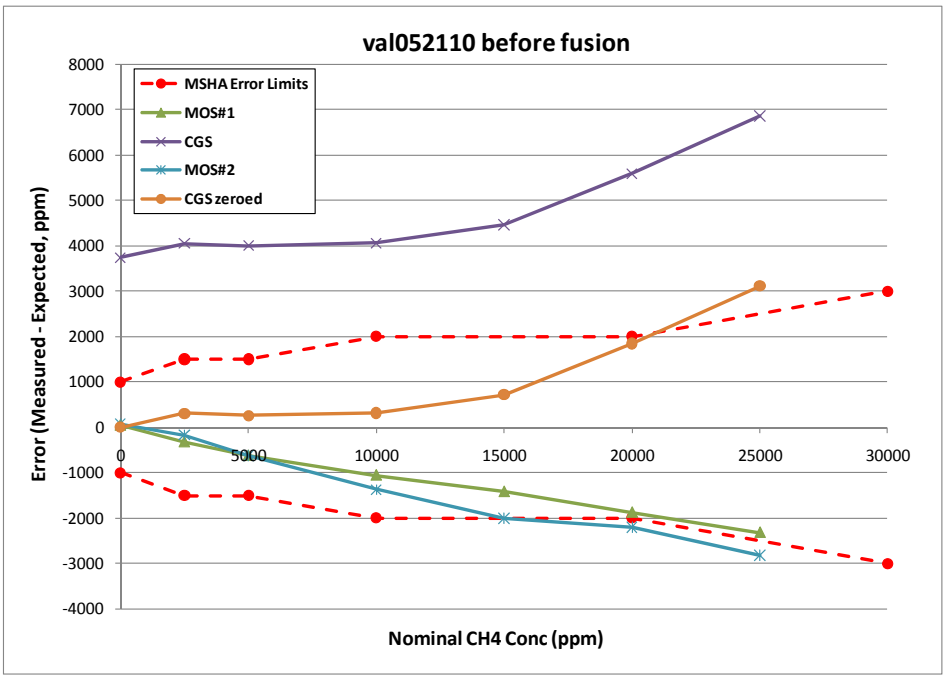

Figure 10e. Errors vs. budget on 05/21/10 for individual redundant CH_4 sensors before data fusion.

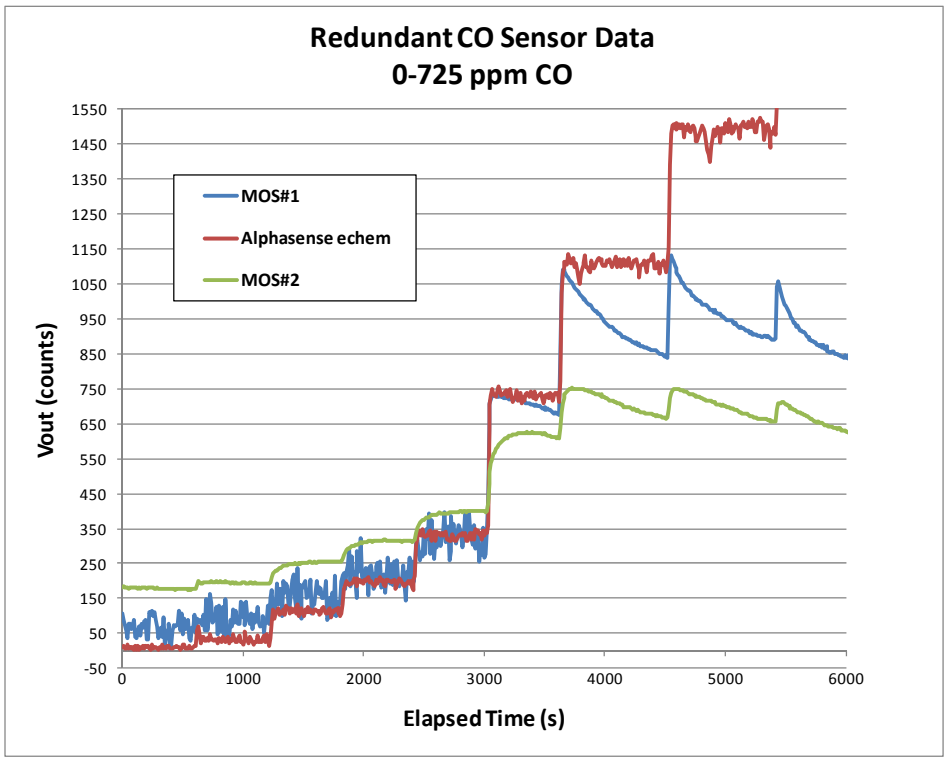

Figure 21. Redundant CO sensor calibration data showing response saturation above ~300 ppm for the MOS sensors. The echem sensor does not have this range limitation.

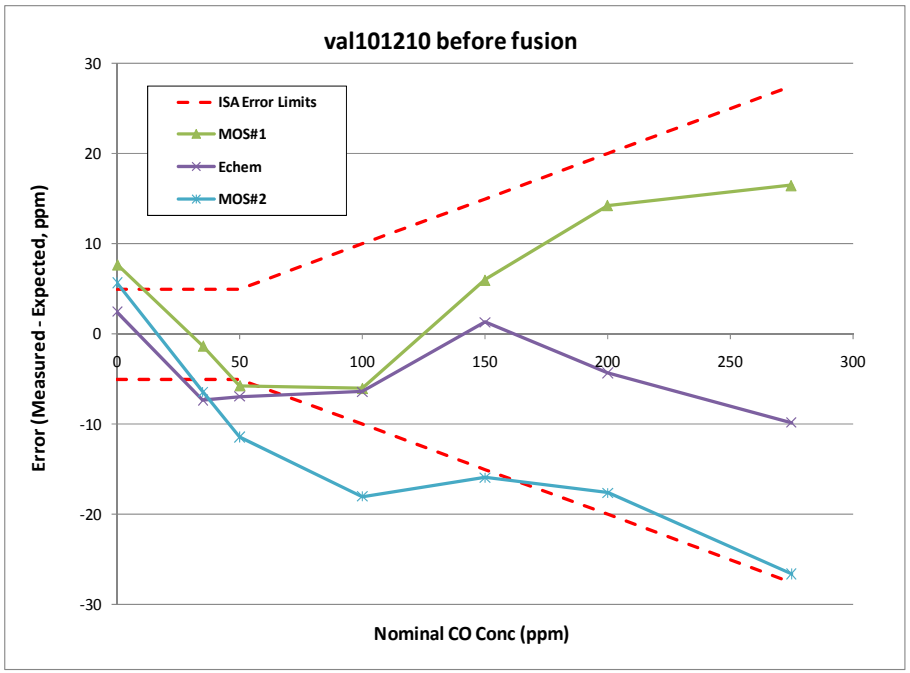

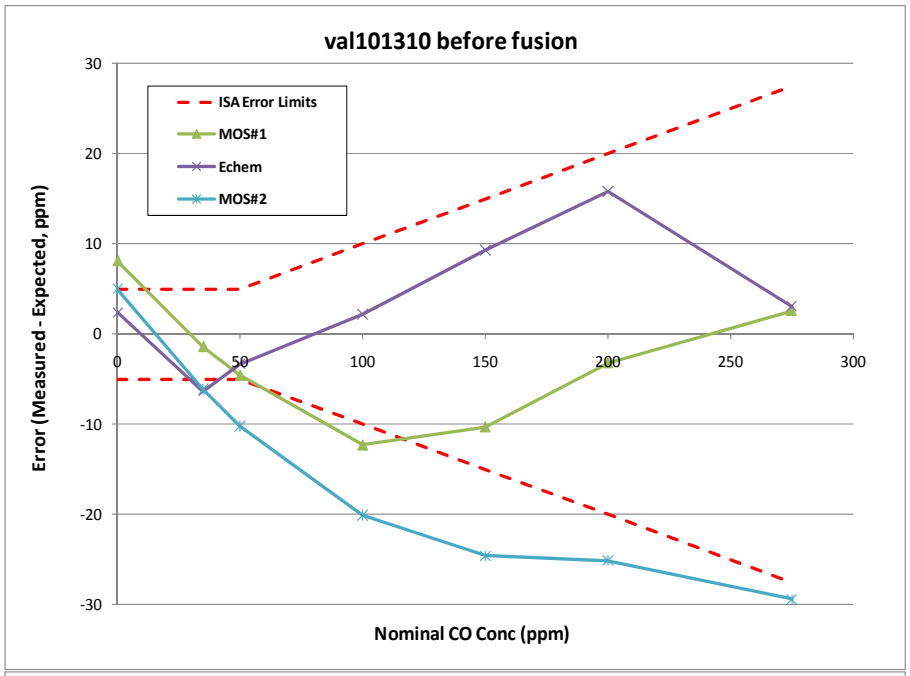

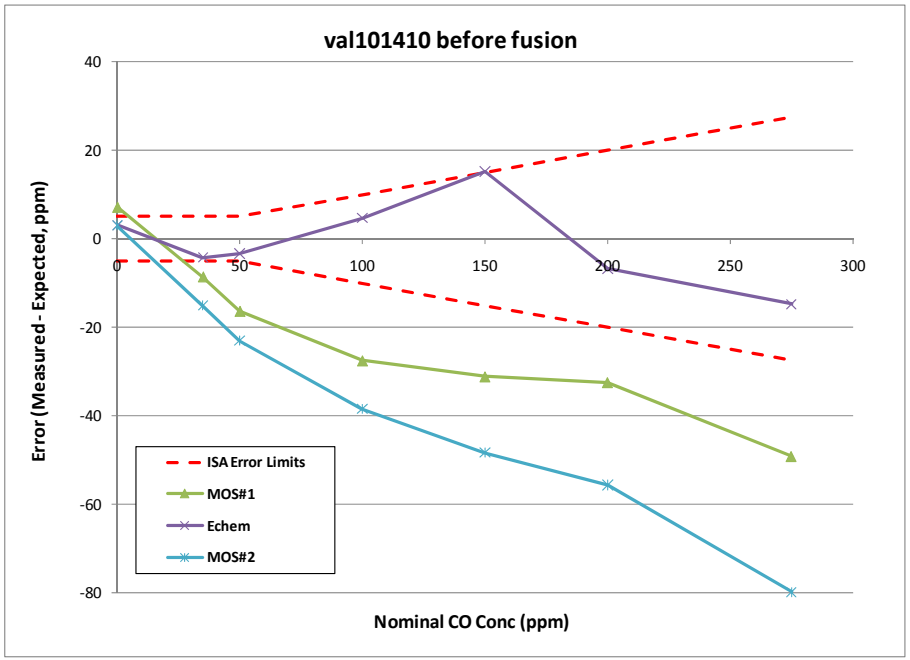

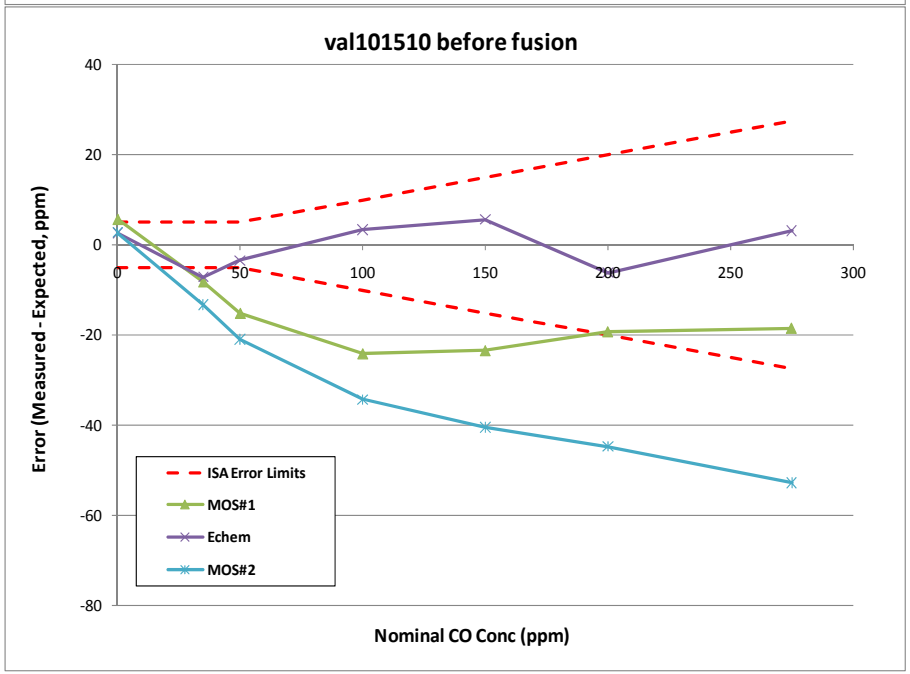

Figure 22a-d. Errors vs. budget for individual redundant CO sensors before data fusion.

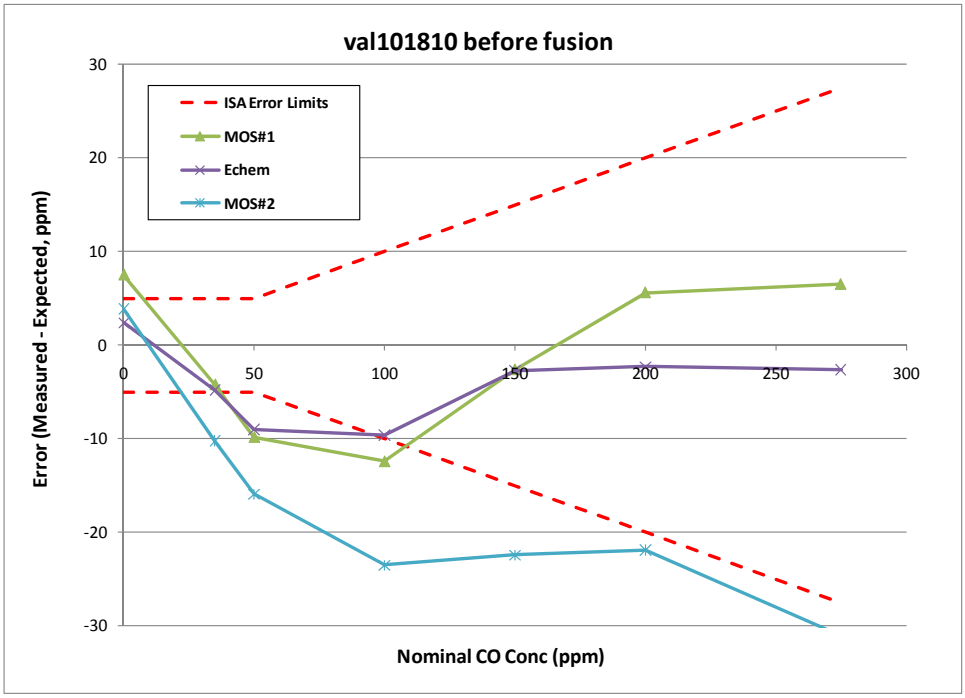

Figure 12e. Errors vs. budget on 10/18/10 for individual redundant CO sensors before data fusion.

Data Fusion Algorithms *(I)*

Data fusion from redundant sensors or distributed multiple sensors is a large and active research area. Although sophisticated methods have been developed (e.g. Kalman filter) for data fusion on a large scale, for small numbers of redundant sensors, simpler weighted average data fusion methods are typically used. There are a number of different weighting schemes that are possible:

1. Arithmetic average (unweighted)
2. Variance weighted average
3. Assigned weights based on prior measurements of individual sensor accuracy vs concentration

After consideration of the characterization of the sensor combinations planned for use on the RS-MG detector, we decided to investigate weighting methods 1 and 3 for the CH_4 sensors. A variance weighted average would essentially give the pellistor sensor a very large weighting relative to the MOS sensors. Although the overall accuracy of the pellistor sensor after zeroing was pretty good, the MOS sensors had lower errors overall.

After inspection of the error trends versus concentration, assignment of 'scaled' weights was made as shown in Table 1. These weights are scaled

Table 1. Assigned weights (scaled versus concentration) used for CH_4 data fusion.

CH4 Conc. (ppm)	MOS Sensor Weight	CGS Sensor Weight
0	1	0
2,500	0.9	0.1
5,000	0.7	0.3
10,000	0.5	0.5
15,000	0.5	0.5
20,000	0.5	0.5
25,000	0.5	0.5

versus concentration, to give much greater weight to the MOS sensors at the lower concentrations with equal weighting above 10,000 ppm. The weights were assigned in this fashion because the MOS sensors tended to have lower errors below 10,000 ppm and a much more stable and accurate zero reading than the pellistor sensor. The better stability and accuracy of the MOS sensor at the low end compared to the pellistor sensor is a combination of the respective pre-amp circuits and the inherent behavior of the sensors themselves. In addition to previously discussed behavior of the Wheatstone bridge circuit for the pellistor sensor described above, the MOS current-to-voltage circuit design tends to minimize the effects of changing sensor baseline resistance, hence resulting in more stable and accurate readings at the low end.

Using the weights from Table 1, the original datasets were post-processed to produce the fused data. Errors in the fused data were then calculated as above. The results obtained after data fusion for the CH_4 tests using methods 1 (no weights) and 3 (scaled weights) are presented in Figure 23 below (fifth dataset not shown due to space). Significant improvement in accuracy was obtained for both data fusion methods, with the majority of the errors now falling within the allowable limits. This improvement in accuracy demonstrates one of the key advantages of the redundant sensor approach. A more quantitative assessment of the improvement in accuracy is discussed in the next section below.

Turning to the redundant CO data, inspection of the error trends versus concentration was used once again in deciding which data fusion methods to investigate. Since the overall performance for the redundant CO sensor types was fairly consistent, the scaled weighting method used above does not apply in this case. Instead, we looked at the variance weighting method (method 2) relative to method 1. This variance weighting method was used successfully by Liao and Chou to improve pH measurement accuracy with a thin-film array of redundant pH sensors [18]. First, variances (unbiased estimates normalized by n-1) from repeat measurements (e.g. the five datasets measured) are calculated for each sensor type at each validation concentration. Then, weights are calculated using these variances as follows:

$$W_{MOS} = v_{CGS} / (v_{MOS} + v_{CGS}) \qquad W_{CGS} = v_{MOS} / (v_{MOS} + v_{CGS}) \tag{1}$$

where W is the weight and v is the variance. The weights obtained are shown in Table 2.

Table 2. Variance weights calculated for the redundant CO sensors (MOS#1 and Echem).

MOS#1	12-Oct	13-Oct	14-Oct	15-Oct	18-Oct	Variance (norm by n-1)	W MOS#1 + Echem
Expected Conc							
0	7.7	8.1	7.2	5.8	7.5	0.8	0.1012
35	33.7	33.6	26.5	26.9	30.8	12.2	0.1358
50	44.3	45.4	33.7	34.9	40.2	28.2	0.1975
100	94	87.7	72.5	75.9	87.6	80.9	0.3380
150	156	139.7	118.9	126.6	147.4	227.4	0.1751
200	214.3	196.8	167.6	180.8	205.6	355.2	0.1995
275	291.5	277.6	225.9	256.6	281.5	679.9	0.0849
Echem							
Expected Conc							
0	2.5	2.4	3.1	2.7	2.4	0.1	0.8988
35	27.7	28.7	30.8	27.9	30.2	1.9	0.8642
50	43.1	46.7	46.7	46.6	41	6.9	0.8025
100	93.6	102.2	104.7	103.4	90.4	41.3	0.6620
150	151.3	159.3	165.2	155.7	147.3	48.3	0.8249
200	195.7	215.8	193.2	193.9	197.7	88.5	0.8005
275	265.2	278.1	260.3	278.2	272.4	63.1	0.9151

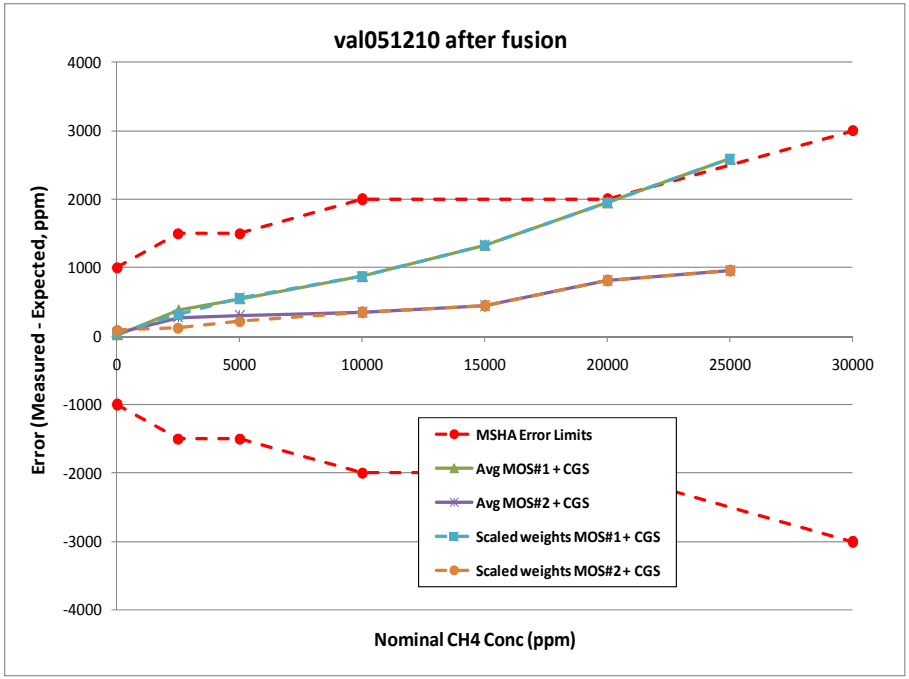

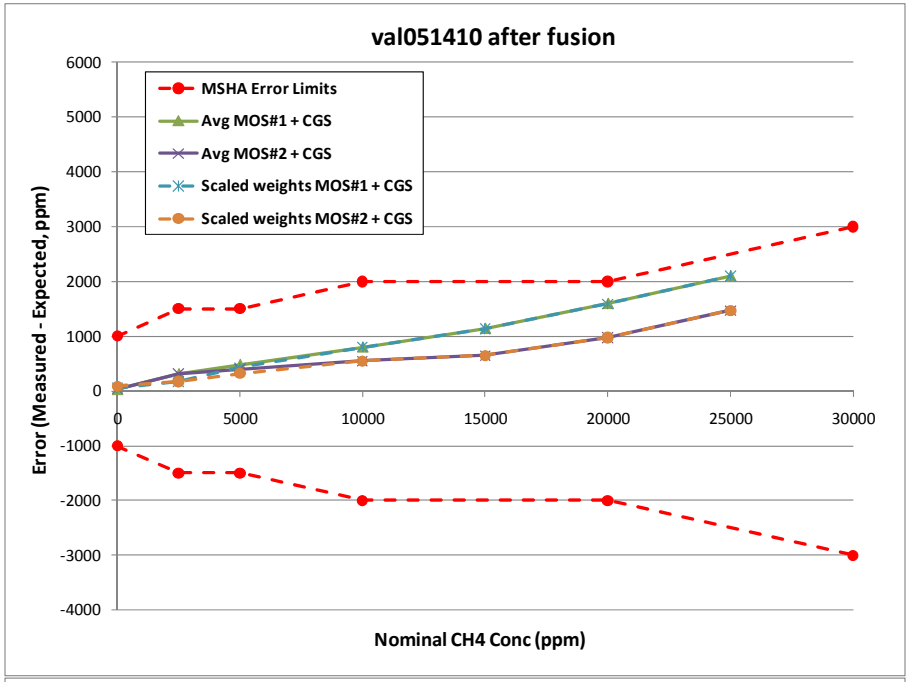

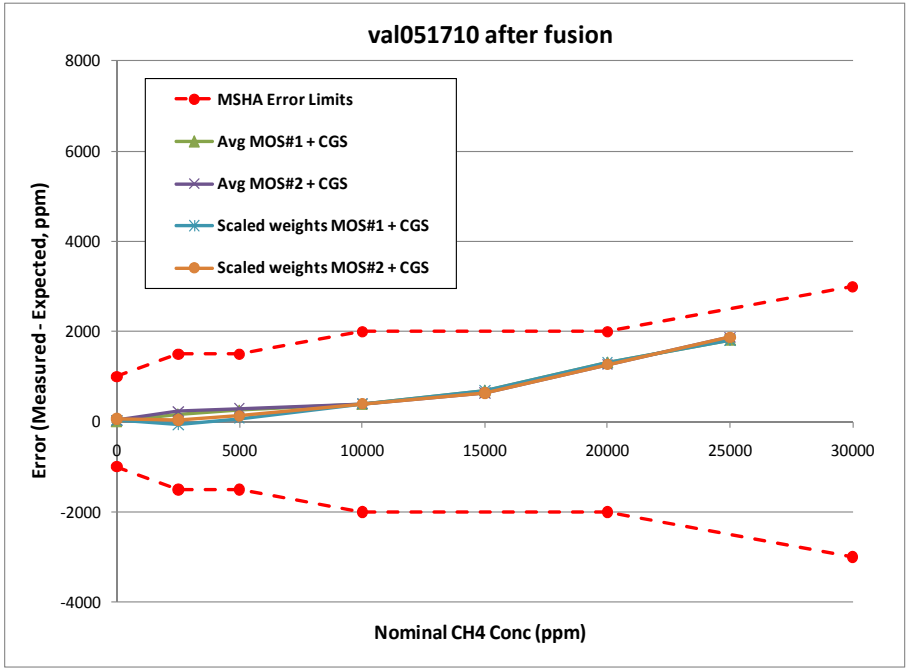

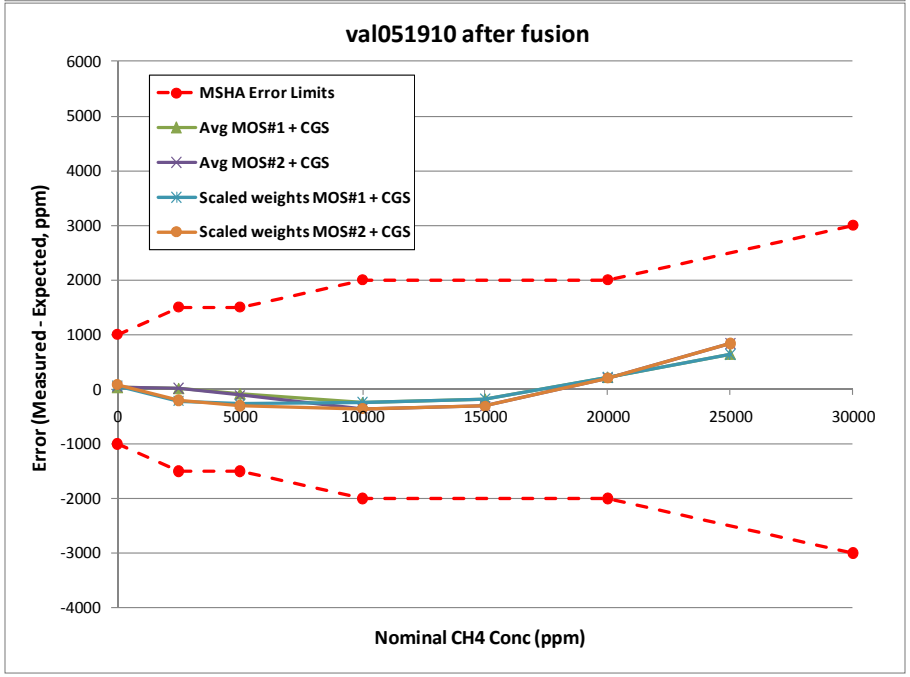

Figure 23a-d. Errors vs. budget for individual redundant CH_4 sensors after data fusion.

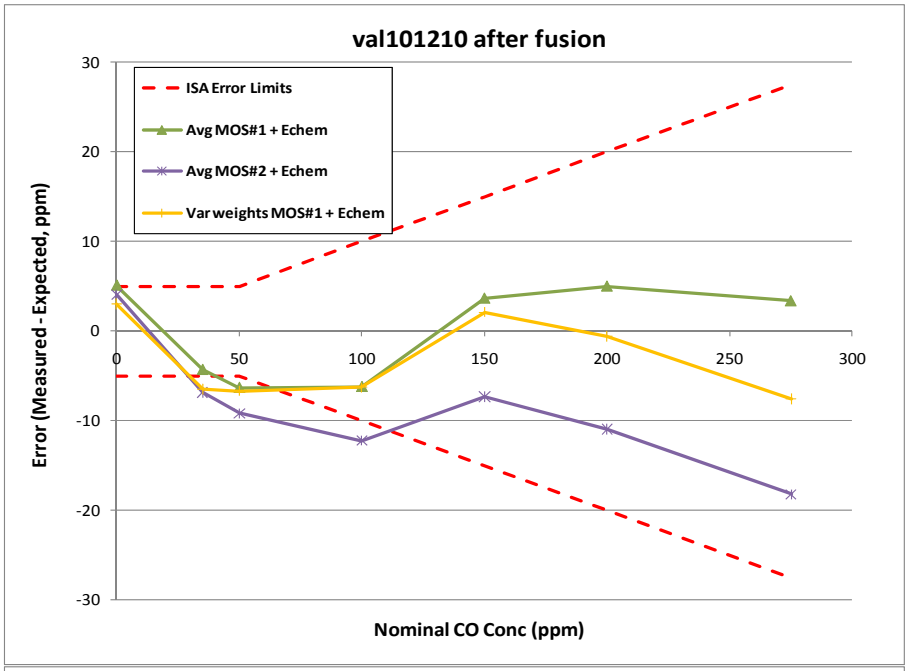

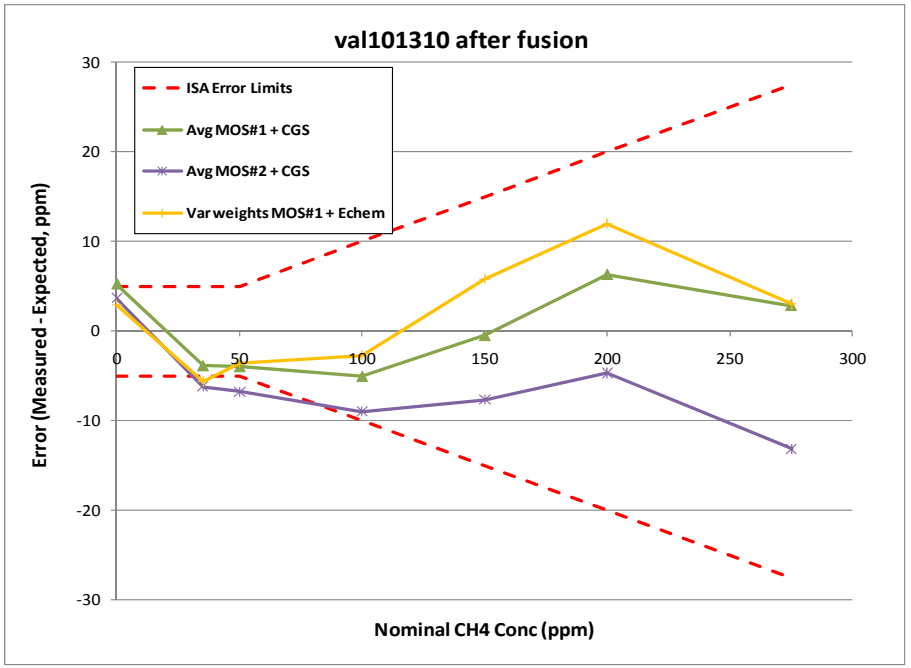

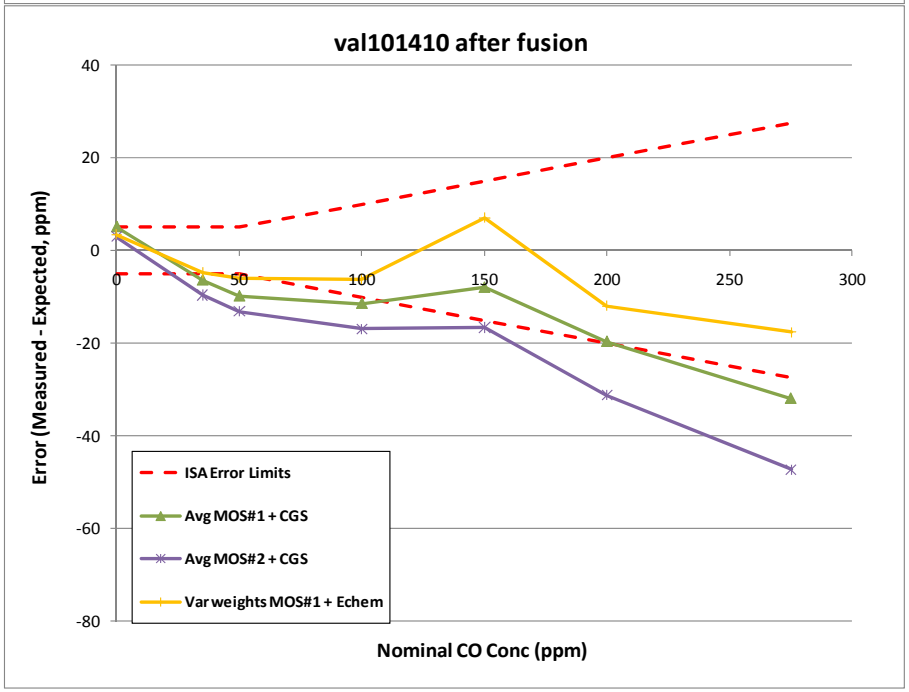

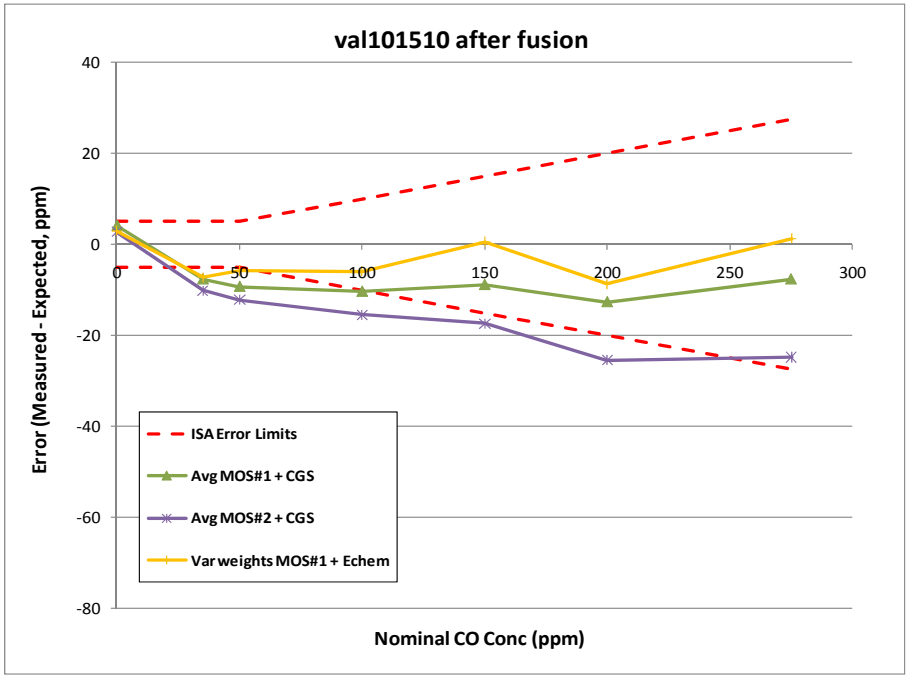

Figure 24a-d. Errors vs. budget for individual redundant CO sensors after data fusion.

The results obtained after data fusion for the CO tests using methods 1 (no weights) and 2 (variance weights) are presented in Figure 24 above (fifth dataset not shown due to space). As with the CH_4 data, both methods led to significant reduction of errors compared to inidivual sensors before data fusion, with the greatest reduction from the variance weighted method. A more quantitative assessment of the improvement in accuracy is discussed in the next section below.

4.5 CONCLUSIONS

Assessment of Data Fusion Results *(I)*

To assist in quantifying, assessing, and comparing the improvements to accuracy obtained from the data fusion methods described above, two metrics were used:

- Chi-squared (sum of squared errors) for all 5 validation datasets (individual and total values)
- # of measurements exceeding error budget for all validation datasets (individual and totals)

These values were determined for all tests and are listed in Table 3 and Table 4, below.

For the CH_4 tests, the scaled weighted average method worked slightly better than the unweighted average in one case (MOS#2 + pellistor) and essentially the same in the other case (MOS#1 + pellistor). The improvement of both fusion methods compared to the individual sensor measurements can clearly be seen for both metrics, but especially in terms of keeping the measurements within the MSHA error budget.

For the CO tests, the improvements from the data fusion can also be seen. In terms of the chi-squared metric, the variance weighted average performs better than the unweighted average, with a total chi-squared value that is 7% lower. Improvement in number of measurements outside the error budget was also seen relative to the MOS sensor readings, but not compared to the echem sensor.

Table 3. Quantitative assessment of data fusion results for CH_4 tests.

						Chi-squared		
Date		**MOS#1**	**CGS zeroed**	**MOS#2**	**Avg MOS#1 + CGS**	**Avg MOS#2 + CGS**	**Scaled weights MOS#1 + CGS**	**Scaled weights MOS#2 + CGS**
05/12/10		2.22E+07	7.36E+06	2.87E+05	1.35E+07	2.07E+06	1.34E+07	1.97E+06
05/14/10		1.58E+07	4.73E+06	3.66E+06	9.19E+06	4.10E+06	9.08E+06	3.97E+06
05/17/10		1.14E+05	2.44E+07	1.32E+05	5.73E+06	5.84E+06	5.64E+06	5.73E+06
05/19/10		7.40E+06	1.34E+07	7.38E+06	5.50E+05	9.69E+05	6.64E+05	1.10E+06
05/21/10		1.26E+07	1.39E+07	1.92E+07	4.50E+05	7.84E+05	6.15E+05	8.96E+05
Totals		**5.80E+07**	**6.38E+07**	**3.06E+07**	**2.94E+07**	**1.38E+07**	**2.94E+07**	**1.37E+07**
						# measurements exceeding budget		
Date		**MOS#1**	**CGS zeroed**	**MOS#2**	**Avg MOS#1 + CGS**	**Avg MOS#2 + CGS**	**Scaled weights MOS#1 + CGS**	**Scaled weights MOS#2 + CGS**
05/12/10		3	0	0	1	0	1	0
05/14/10		2	0	0	0	0	0	0
05/17/10		0	2	0	0	0	0	0
05/19/10		0	1	0	0	0	0	0
05/21/10		0	1	3	0	0	0	0
Totals		**5**	**4**	**3**	**1**	**0**	**1**	**0**
Red is highest value for each dataset. Green is lowest value (best result) for each dataset.								

Table 4. Quantitative assessment of data fusion results for CO tests.

					Chi-squared		
Date		**MOS#1**	**Echem**	**MOS#2**	**Avg MOS#1 + Echem**	**Avg MOS#2 + Echem**	**Var weights MOS#1 + Echem**
10/12/10		642	264	1798	172	801	197
10/13/10		363	407	2670	132	431	249
10/14/10		5574	554	14030	1758	4038	610
10/15/10		2163	161	8196	565	2054	207
10/18/10		404	221	2873	268	1083	237
Totals		**9.15E+03**	**1.61E+03**	**2.96E+04**	**2.89E+03**	**8.41E+03**	**1.50E+03**
					# measurements exceeding budget		
Date		**MOS#1**	**Echem**	**MOS#2**	**Avg MOS#1 + Echem**	**Avg MOS#2 + Echem**	**Var weights MOS#1 + Echem**
10/12/10		2	2	5	1	3	2
10/13/10		2	1	6	1	2	1
10/14/10		7	1	6	5	6	1
10/15/10		5	1	6	3	5	2
10/18/10		3	1	6	2	3	2
Totals		**19**	**6**	**29**	**12**	**19**	**8**
Red is highest value for each dataset. Green is lowest value (best result) for each dataset.							

Benefits of Redundant Sensors for Gas Detection

Users of safety instrumentation in many industries have continually expressed concerns over sensor reliability, especially in terms of accuracy and false negative and positive alarms. The results presented above show the clear benefits of Synkera's redundant sensor approach in terms of improved sensor accuracy, measurement range, and reduction of baseline drift. Although the scope of the tests presented above was limited in terms of numbers of sensors and tests, the results clearly shown the great potential for the redundant sensor approach to multi-gas monitoring for mine safety applications. A number of other benefits of the redundant sensor approach to multi-gas monitoring for mine safety applications have been discussed in previous sections as well. In this project, Synkera has used various sensor types, good detector design, and data fusion methods, to demonstrate a groundbreaking technology for improving the reliability of multi-gas detection for mine safety. With further development work and successful deployment of this technology, the personal safety of mine workers around the world will be enhanced resulting in reduction of personal injuries and loss of life.

References Cited

1. U.S. Bureau of Labor Statistics, U.S. Department of Labor, 2007
2 Code of Federal Regulations, Title 30 CFR Part 75.
3. G.E. Thompson and G.C. Wood, in J.C. Scully (Ed.), Corrosion: Aqueous Processes and Passive Films, Academic, London, (1983).
4. D. Routkevich, et al, *IEEE Trans. Electron Dev.,* 43(10), 1646-1658 (1996).
5. D. Routkevitch *et al*, Nanostructured Ceramic Platform for Micromachined Devices and Device Arrays**, US patent** No 6,705,152 B2, 03/16/04
6. E2V website: http://e2vtechnologies.com.
7. City Technology website: http://www.citytech.com.
8. Chu, PP; Reddy, MJ, "Sm2O3 composite PEO solid polymer electrolyte", J. Power Sources 2003, 115(2), 288-294.
9. Jin, Z., et al., "Application of Nano-Crystalline Porous Tin Oxide Thin Film for CO Sensing," Sensors and Actuators B 1998, 52, 188-194.
10. Bose, A.C. et al, "Grain size dependent electrical studies on nanocrystalline SnO_2", Materials Chemistry and Physics 2006, 95, 72-78.
11. Wu, N.L., Wang, S.Y., and Rusakova, I.A., "Inhibition of Crystallite Growth in the Sol-Gel Synthesis of Nanocrystalline Metal Oxides," Science 1999, 285, 137-9.
12. Nanostructured Electrochemical Ozone Monitors, NIEHS SBIR Phase I Grant 1 R43 ES017192-01, PI: C.J. Kostelecky
13 Novel Hydrogen Sulfide Sensors for Portable Monitors, CDC Grant H07471, SBIR Phase II. PI: S.S. Williams.
14 A. Govyadinov, P. Mardilovich, K. Novogradecz, S. Hooker, D. Routkevitch, Anodic Alumina MEMS: Applications and Devices, *Proc. MEMS-2000,* Vol. 2, 313-318 (2000).
15. P. Mardilovich, A. Govyadinov, D. Routkevitch, Proc. of the 198th Meet. Electrochem. Soc., Oct. 23-27 2000-19, 33-42, 2000.
16. Advanced personal gas detectors for mining applications, NIOSH Phase I SBIR GRANT 1 R43 OH009026-01, and Phase II grant 5R44OH009026-03, PI: D. Routkevitch
17 R. Dagavi, Putting the "Nano" into Composites, Chem. Eng. News, **77**, #23, p. 25-37 (1999)
18 Liao, Y. and Chou, J., "Weighted Data Fusion Use for Ruthenium Dioxide Thin Film pH Array Electrodes", IEEE Sensors Journal, Vol. 9, No. 7, July 2009.